Progress in Oceanography 80 (2009) 22–50

Contents lists available at ScienceDirect

Progress in Oceanography

journal homepage: www.elsevier.com/locate/pocean

Geological and biological heterogeneity of the Aleutian margin (1965–4822 m)

A.E. Rathburn [a,b,*], L.A. Levin [b], M. Tryon [c], J.M. Gieskes [b], J.B. Martin [d], M.E. Pérez [a,e], F.J. Fodrie [b,2], C. Neira [b], G.J. Fryer [f,1], G. Mendoza [b], P.A. McMillan [b], J. Kluesner [a,3], J. Adamic [a], W. Ziebis [g]

[a] Indiana State University, Geology Program, 179 Science Bldg., Terre Haute, IN 47809, USA
[b] Scripps Institution of Oceanography, Integrative Oceanography Division, La Jolla, CA 92093-0218, USA
[c] Scripps Institution of Oceanography, Geosciences Research Division, La Jolla, CA 92093-0244, USA
[d] University of Florida, Dept. Geological Sciences, Gainesville, FL 32611-2120, USA
[e] The Natural History Museum, Micropaleontology, Cromwell Road, London SW7 5BD, UK
[f] School of Ocean & Earth Science & Technology, University of Hawaii at Manoa, Honolulu, HI 96822, USA
[g] Department of Biological Sciences, University of Southern California, Los Angeles, CA 90089-371, USA

ARTICLE INFO

Article history:
Received 1 March 2008
Received in revised form 21 November 2008
Accepted 5 December 2008
Available online 25 December 2008

Keywords:
Alaska
Aleutian margin
Biogeochemistry
Benthic biota
Disturbance
Diversity
Canyons
Cold seeps

ABSTRACT

Geological, biological and biogeochemical characterization of the previously unexplored margin off Unimak Island, Alaska between 1965 and 4822 m water depth was conducted to examine: (1) the geological processes that shaped the margin, (2) the linkages between depth, geomorphology and environmental disturbance in structuring benthic communities of varying size classes and (3) the existence, composition and nutritional sources of methane seep biota on this margin. The study area was mapped and sampled using multibeam sonar, a remotely operated vehicle (ROV) and a towed camera system. Our results provide the first characterization of the Aleutian margin mid and lower slope benthic communities (microbiota, foraminifera, macrofauna and megafauna), recognizing diverse habitats in a variety of settings. Our investigations also revealed that the geologic feature known as the "Ugamak Slide" is not a slide at all, and could not have resulted from a large 1946 earthquake. However, sediment disturbance appears to be a pervasive feature of this margin. We speculate that the deep-sea occurrence of high densities of *Elphidium*, typically a shallow-water foraminiferan, results from the influence of sediment redeposition from shallower habitats. Strong representation of cumacean, amphipod and tanaid crustaceans among the Unimak macrofauna may also reflect sediment instability. Although some faunal abundances decline with depth, habitat heterogeneity and disturbance generated by canyons and methane seepage appear to influence abundances of biota in ways that supercede any clear depth gradient in organic matter input. Measures of sediment organic matter and pigment content as well as C and N isotopic signatures were highly heterogeneous, although the availability of organic matter and the abundance of microorganisms in the upper sediment (1–5 cm) were positively correlated.

We report the first methane seep on the Aleutian slope in the Unimak region (3263–3285 m), comprised of clam bed, pogonophoran field and carbonate habitats. Seep foraminiferal assemblages were dominated by agglutinated taxa, except for habitats above the seafloor on pogonophoran tubes. Numerous infaunal taxa in clam bed and pogonophoran field sediments and deep-sea "reef" cnidarians (e.g., corals and hydroids) residing on rocks near seepage sites exhibited light organic $\delta^{13}C$ signatures indicative of chemosynthetic nutritional sources. The extensive geological, biogeochemical and biological heterogeneity as well as disturbance features observed on the Aleutian slope provide an attractive explanation for the exceptionally high biodiversity characteristic of the world's continental margins.

1. Introduction

The world's continental margins are highly heterogeneous environments. Geomorphic features such as submarine canyons, gullies, terraces, hills and scarps criss-cross the slope, reflecting erosional, depositional and tectonic processes. Additionally, geochemical features associated with methane seeps, brine pools or organic depo-centers create a mosaic of microbial and faunal hotspots interwoven across the margin landscape. All of these features

* Corresponding author. Address: Indiana State University, Geology Program, 179 Science Bldg., Terre Haute, IN 47809, USA. Tel.: +1 8122372269.
E-mail address: arathburn@isugw.indstate.edu (A.E. Rathburn).
[1] Present address: Pacific Tsunami Warning Center, 91-270 Fort Weaver Rd., Ewa Beach, HI 96706-2928, USA.
[2] Present address: Dauphin Island Sea Laboratory, 101 Bienville Blvd., Dauphin Island, Al 36528, USA.
[3] Present address: Scripps Institution of Oceanography, Geosciences Research Division, La Jolla, CA 92093-0244, USA.

0079-6611/$ - see front matter © 2008 Elsevier Ltd. All rights reserved.
doi:10.1016/j.pocean.2008.12.002

have been identified on the North American margin. Although studies have examined the resulting habitats separately (e.g., Vetter, 1995; Hecker et al., 1983), rarely have their combined influences on benthic community structure and geochemistry been examined holistically and in close proximity. This is especially true in remote regions such as the margin off the Aleutian Islands in the North Pacific where much of the deep-sea floor remains virtually unexplored. As a result, detailed seafloor charts are lacking and relatively little is known about the mosaic of geological and biological features in the region.

The Alaskan margin consists of a suite of highly dynamic environments, influenced by tectonic activity, biogeochemical processes and the influx of organic material from shallow water and sediment subsurface sources. Temporal and spatial variability in environments combine to appreciably influence benthic communities. Some of this variability is brought about by disturbances associated with mass wasting events, such as turbidity currents and slides, and the consequent initiation of cold methane seeps through erosion of overburden above methane sources or entrapment of sufficient organic material for subsequent methane production. We focused our research on the slope off Unimak Island in the Aleutian chain because this sector of the margin had been proposed as the site of a submarine slide that caused a 1946 tsunami that had lethal effects in both Alaska and Hawaii. Based on GLORIA images of the region (Dobson et al., 1996), a potential slide was identified off the coast of Unimak Island. The projected size and location of the feature was consistent with some models of tsunami characteristics, and was considered as a probable source of the displacement that caused the tsunami in 1946 (Fryer et al., 2004).

In July 2004 we mapped and sampled the margin off Unimak Island, Alaska between 1965 m and 4822 m water depth using multibeam sonar, a remotely operated vehicle (ROV) and a towed camera system (Fig. 1a–h). The goals of this study were to: (1) map this relatively unexplored area of the Aleutian margin to characterize geological features and identify marine benthic habitats; (2) examine the relationships between seafloor communities and environmental parameters, including disturbance; (3) characterize the abundance and composition of epifaunal and infaunal communities living on the margin, and (4) examine interactions among biology, geology and geochemistry in generating the mosaic of habitats present along this active margin. This research provides the first holistic characterization of the Gulf of Alaska slope benthic communities, recognizing diverse habitats in a variety of settings.

Through an integrated analysis of the geology, geochemistry, biogeochemistry and biology of deep-sea environments, we addressed the following hypotheses on the Aleutian margin off the coast of Unimak Island. (1) The geology of the area was distinctly influenced by the 1946 earthquake, with a landslide disturbance signature evident in seafloor morphology and biology; and (2) the study area is inhabited by a mosaic of benthic assemblages that are influenced by physical and geochemical habitat heterogeneity, including features such as topography, water depth, organic matter availability and methane seepage. We targeted a broad size-spectrum of benthic biota including the epibenthic megafauna visible in bottom photographs, macroinfaunal invertebrates (animals collected in small cores and retained on a 0.3 mm mesh) and foraminifera.

2. Background – Aleutian margin off Unimak Island

The segment of the Aleutian Trench offshore of Unimak Island marks the transition from Pacific Plate subduction beneath the continental lithosphere of Alaska and the Alaskan Peninsula to subduction beneath the volcanic arc of the Aleutian Islands and the oceanic lithosphere of the Bering Sea. Plate convergence is roughly perpendicular to the bathymetric trend of the trench at a rate of about 6.7 cm yr^{-1} (DeMets and Dixon, 1999). The region was partly surveyed in the 1980s (Lewis et al., 1988) and later imaged with GLORIA (Dobson et al., 1996). The morphology of the area below the shelf break can be divided into three distinct morpho-tectonic regions extending along strike of the trench axis. The midslope region above ~2500 m is dominated by sediment transport processes with a deeply incised canyon morphology with a thick sediment drape. The midslope Aleutian Terrace is a series of deep forearc basins bounded by prominent and laterally extensive trenches parallel to anticlinal ridges and uplifted blocks that collect most of the sediment from the upper slope. The terraced lower trench slope below ~4200 m is a highly faulted prism with morphology that is largely controlled by trench parallel thrust and normal faulting with an overprinting of WNW trending right-lateral strike slip faults, often extending across the entire slope. Sediment supply to the area was likely rapid during glacial low stands. However, sediment supply is now comparatively reduced and slope failure is the primary process generating sediments to the area (Dobson et al., 1996). The area exhibits frequent, strong seismic activity that likely triggers slumps and debris flows and produces the broad amphitheaters at the heads of canyons that are evident in the bathymetric images. A very large feature on the slope south of Unimak Island was tentatively identified, based on GLORIA imagery, as the toe of a landslide resulting from the April 1, 1946 M_s 7.1 earthquake event offshore of Unimak Island (Fryer et al., 2004).

Much of what was previously known of the seafloor biology and geology of the region was based on only 3 cores and remote surveys. Remote surveys were conducted on the Aleutian margin (Lewis et al., 1988) and in the Gulf of Alaska (Suess and Bohrmann, 1997), and Wallmann et al. (1997) examined the geochemistry of seeps east of Kodiak Island in the Gulf of Alaska. Macrofauna were studied from the Aleutian Trench by Belyaev (1966) (2 cores) and Jumars and Hessler (1976) (1 core) from depths between 6460 and 7298 m. Jumars and Hessler (1976) noted unusually high macrofaunal density (1272 ind m^{-2}) and low diversity for hadal depths. They attributed these observations to sediment instability, and productive overlying waters. Levin and Mendoza (2007) examined the community structure and nutrition of infaunal seep taxa from the Aleutian margin, and Basak et al. (2009) reported stable isotope and distribution data for one foraminiferal taxon from the region. We know of no other studies of deep Aleutian margin macrofauna, microbiota or foraminifera.

3. Materials and methods

3.1. Field sampling

During a cruise aboard the *R/V Roger Revelle* in July 2004, we used shipboard sonar, the ROV Jason II and a towed camera system (Tow Cam) to map the Aleutian margin adjacent to Unimak Island, Alaska (near 53°30N 164°00W). Seafloor photographs were obtained during four Tow Cam camera image surveys and biological, geological and geochemical samples were obtained from seven Jason II dives. Jason II manipulators collected seafloor samples from nine stations on the Unimak margin (Table 1) using tube cores (8.3 cm diameter × 20 cm deep), sediment scoop bags (upper 5–10 cm of sediment), a slurp gun and direct collection of rocks. A diverse array of habitats was examined (Fig. 2a–d). The stations (Fig. 1a–g) included three canyon floors (1965 m, 3600 m, 4620 m), an elevated mid-basin block isolated from the main slope (3190 m), a deep scarp base (4822 m), a midslope terminal escarpment (3580–4240 m), the open slope (3310 m) and two

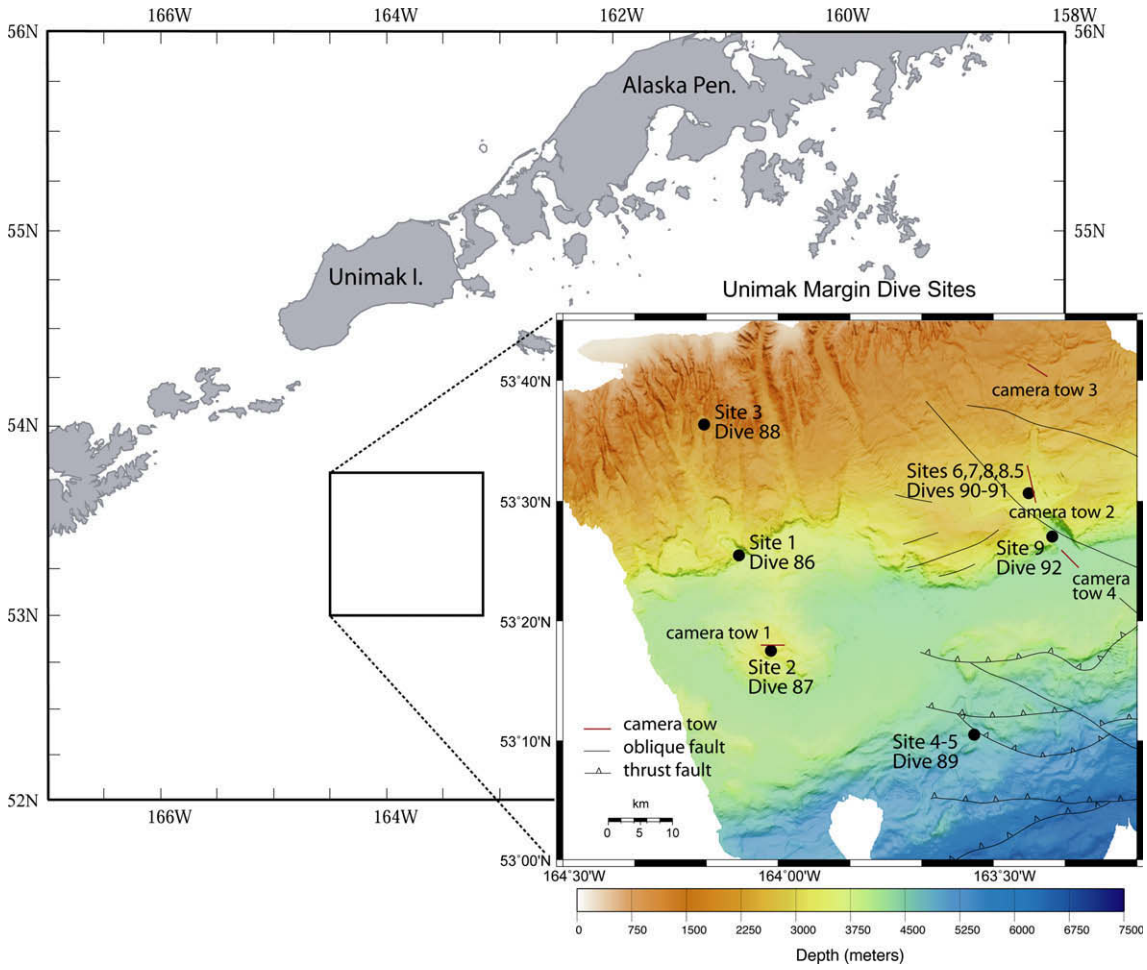

Fig. 1. Maps. (a) Site map showing regional context with the sampling sites and dive numbers indicated; (b–g) Detailed bathymetry, dive tracks, site locations and camera tow transects (Camera Tow 1 is shown in detail in (c); Camera Tow 2 is shown in detail in (f); Camera Tow 3 is only shown in (a); Camera Tow 4 is shown in detail in (g); (h) bathymetry and structural interpretation of the region. Previously proposed Ugamak Slide is indicated as are the sites described in the text. Structural interpretation is from Lewis et al. (1988). The lack of interpretation in the western region is due to an absence of available sub-bottom imaging.

methane seep habitats: vesicomyid clam beds (Fig. 2a; 3267–3277 m), and an adjacent pogonophoran field (Fig. 2c; 3283 m). From each sampling site we collected replicate tube cores for analyses of porewater and sediment geochemistry, foraminifera and macrofauna (>0.3 mm). Ship board analyses included core imaging by X-radiography, geochemical microprofiling of cores, core sub-sampling for porewater and sediment geochemistry, core processing for microbiological studies, meiofauna and macrofauna community analysis, sub-sampling of rock samples and microscopic examination of selected samples and specimens. Total organic carbon (TOC), total nitrogen (TN), chlorophyll *a* (chl *a*), phaeopigments, chloroplastic pigment equivalents (CPE, i.e., sum of chl *a* and phaeopigments) and natural abundance of stable isotopes $\delta^{13}C$ and $\delta^{15}N$, were determined from surface sediments (0–1 cm). X-ray samples (Fig. 3a–h) and digital sediment images (Fig. 4a–e) were taken with a plexiglass slab inserted into the tubecore immediately upon recovery. Samples of rock epifauna were collected with the ROV manipulator from carbonate and non-carbonate rocks. These were returned in a sealed biobox, photographed on the ship and frozen (−80 °C) for stable isotope analyses ($\delta^{15}N$, $\delta^{13}C$).

3.2. Bathymetric mapping

A bathymetric survey was conducted aboard the *R/V Roger Revelle* between approximately 163° and 164.5°W from the shelf break to the trench using the Kongsberg Simrad EM120 12 kHz, 191-beam, 150° swath mapping system. Sippican MK-12 XBTs were used as needed for velocity correction and the acquired data were processed with MB-System (Caress and Chayes, 1995, 1996) and visualized using GMT (Wessel and Smith, 1991). Track width and resolution varied greatly due to the extreme depth range, further, the system was not in prefect tune, so effective horizontal resolution at the greater depths was probably only 50 m. To avoid artifacts, the bathymetry on which our maps are based was gridded at 100 m. The area of our survey east of 163°40′ was the subject of a 1984 multibeam and single-channel seismic survey (Lewis et al., 1988) which we have used to interpret some of the large-scale structural features of the area (Fig. 1h).

3.3. Camera Tow surveys and photo analysis

Bottom-photo and video transects documented the location and distribution of biological and geological features including the distribution of megafauna (animals visible in camera sled photographs; typically >1 cm) and the occurrence of hardgrounds. Seabed photographs were obtained over four transects in the study region: across the summit of the Mid-basin block at about 3200 m (Tow 1; Fig. 1c), along the slope at about 3200 m (Tow 2; Fig. 1f) and about 2000 m (Tow 3; Fig. 1a), and over the terrace basin near the Canyon Mouth Fault at about 4200 m (Tow 4; Fig. 1g). Photo-transects were made using Woods Hole Oceanographic

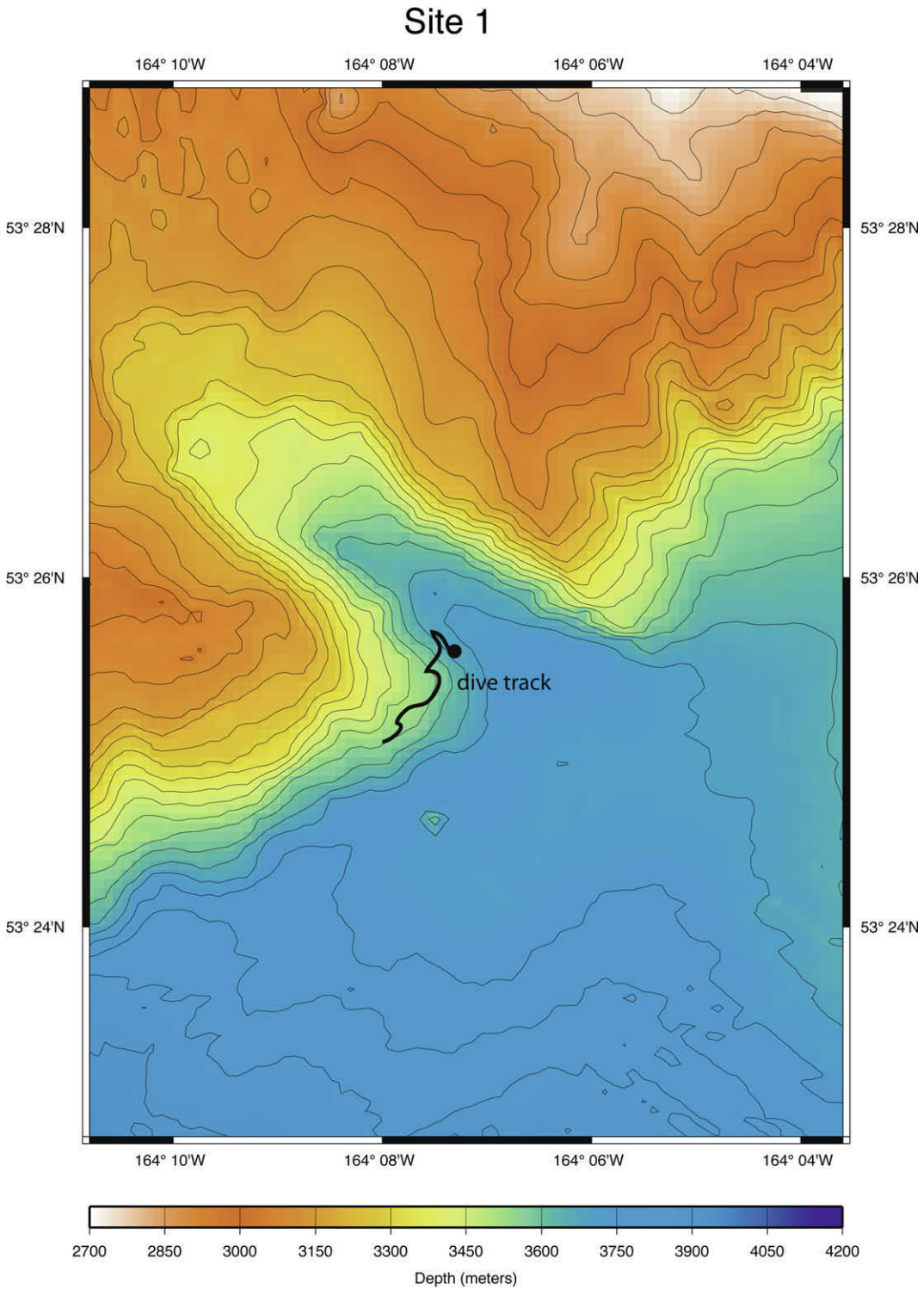

Fig. 1b. Detailed bathymetry and dive track for Site 1.

Institution's Tow Cam that consists of a downward-facing internally recording digital camera with two oblique strobes. Each tow lasted approximately 4 h from deployment to recovery, and the system was set to record seabed photos every 10 s once the system reached bottom. Bottom transects stretched between 7.2 and 10.2 km in length, and between 1200 and 1800 bottom photos were captured during each tow (Fig. 1a and Table 2).

Following system recovery, digital bottom photographs were imported in to Adobe Photoshop 5.0 for analysis. Three to six serial photos could overlap the same seafloor, and therefore we only analyzed every 10–15th (randomly determined) photo to quantify community composition. Each image was divided into a 3×3 grid, and each grid cell was enlarged to aid in identification. Organisms were classified to the lowest taxonomic level possible, and entered into a database. Identification was aided by comparison of images to specimens collected during Jason II dives. Using bottom features such as holes and man-made debris, we concluded that our resolution was approximately 2 cm. Using the system's altitude, it was

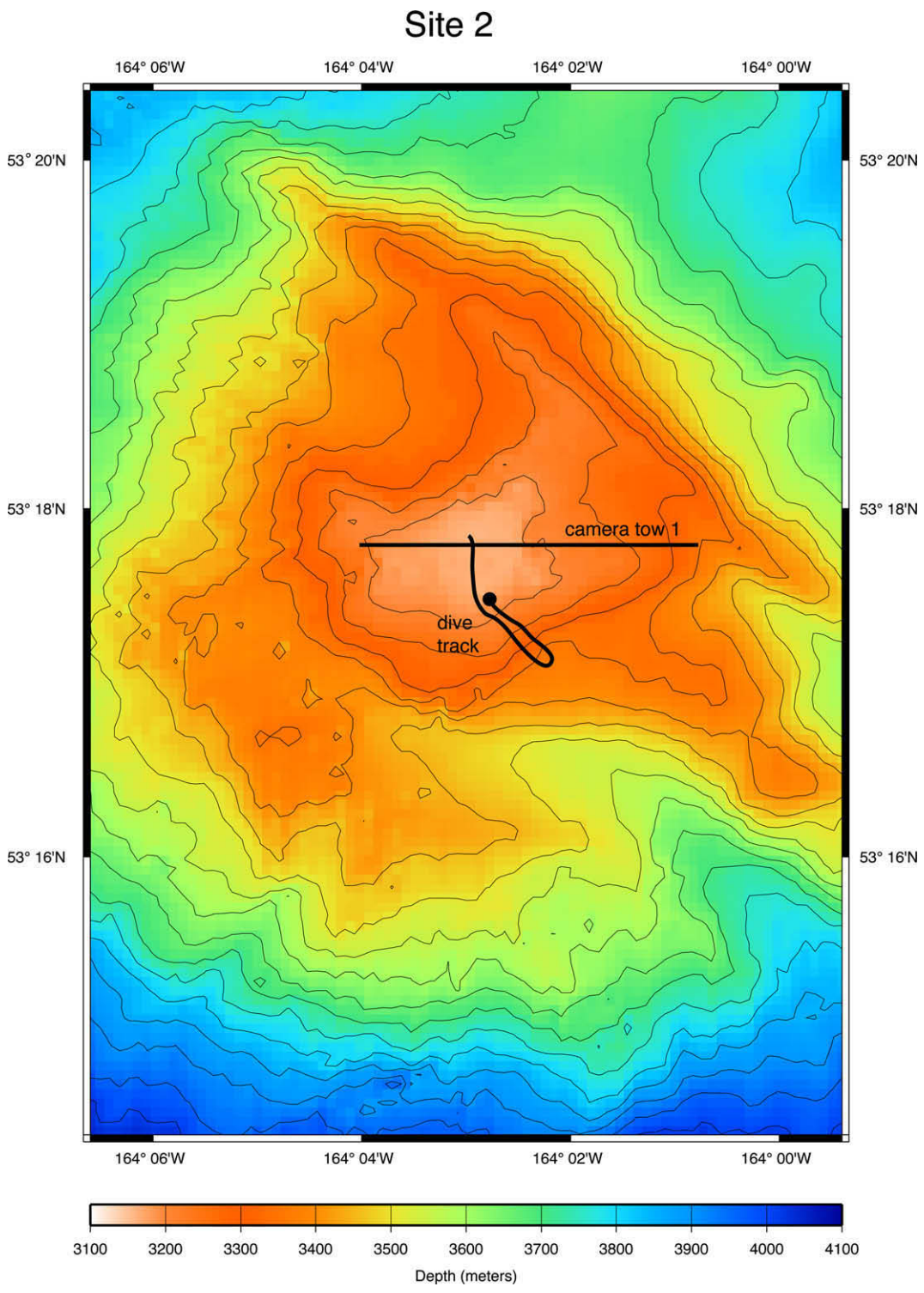

Fig. 1c. Detailed bathymetry, and dive track and camera tow 1 of Site 2.

possible to calculate the area of bottom visible in the photos, and therefore megafaunal densities. We investigated differences in megafaunal densities using ANOVA (at the phyla level) and Kruskal–Wallis (below the phyla level, where zeros dominated the dataset) tests on untransformed data, in which transect was considered fixed. Additionally, we explored patterns of megafaunal community similarity/dissimilarity among photo transects using multidimensional scaling (MDS).

3.4. X-radiography

Sediment structures within selected tube cores were imaged on board ship using X-radiography by means of an ACOMA (Kramex) model PX-20N portable X-ray unit. One or two replicate slabs of sediment were collected from cores with a plexiglass subcorer ($1 \times 7 \times 15$ and 17×21 cm deep). Sediment slabs were stored in the cold room for several hours, then outer slab walls were cleaned

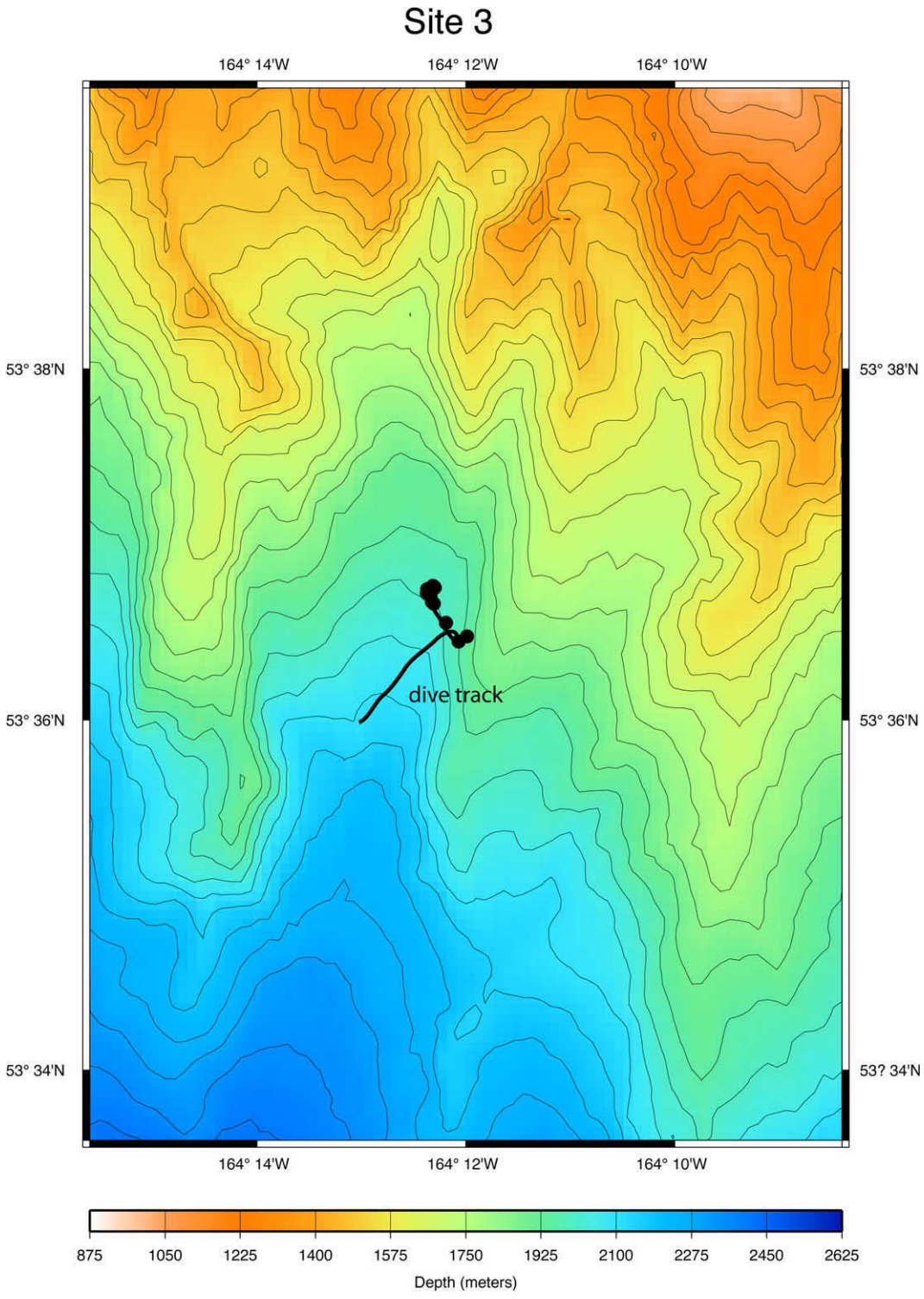

Fig. 1d. Detailed bathymetry and dive track of Site 3.

and X-radiographs were taken and developed on board the ship. To examine external visual features of the sediment column (e.g., color, gradient of bulk density and biogenic structures), color images were photographed directly from the same slabs used for X-ray, with a Nikon digital camera (Coolpix 995, 3.3 MP) at a distance of 50 cm. Resultant X-radiographs were also photographed with a digital camera and resolution quality of all images (X-ray and photographic) was improved with Photoshop software.

3.5. Geochemistry

The undisturbed cores taken by the ROV Jason II allowed for high-resolution measurements and detailed sub-sampling. Microelectrode profiles in combination with the porewater and sediment analyses were used to characterize the subsurface geochemistry of different environments for comparisons with faunal parameters.

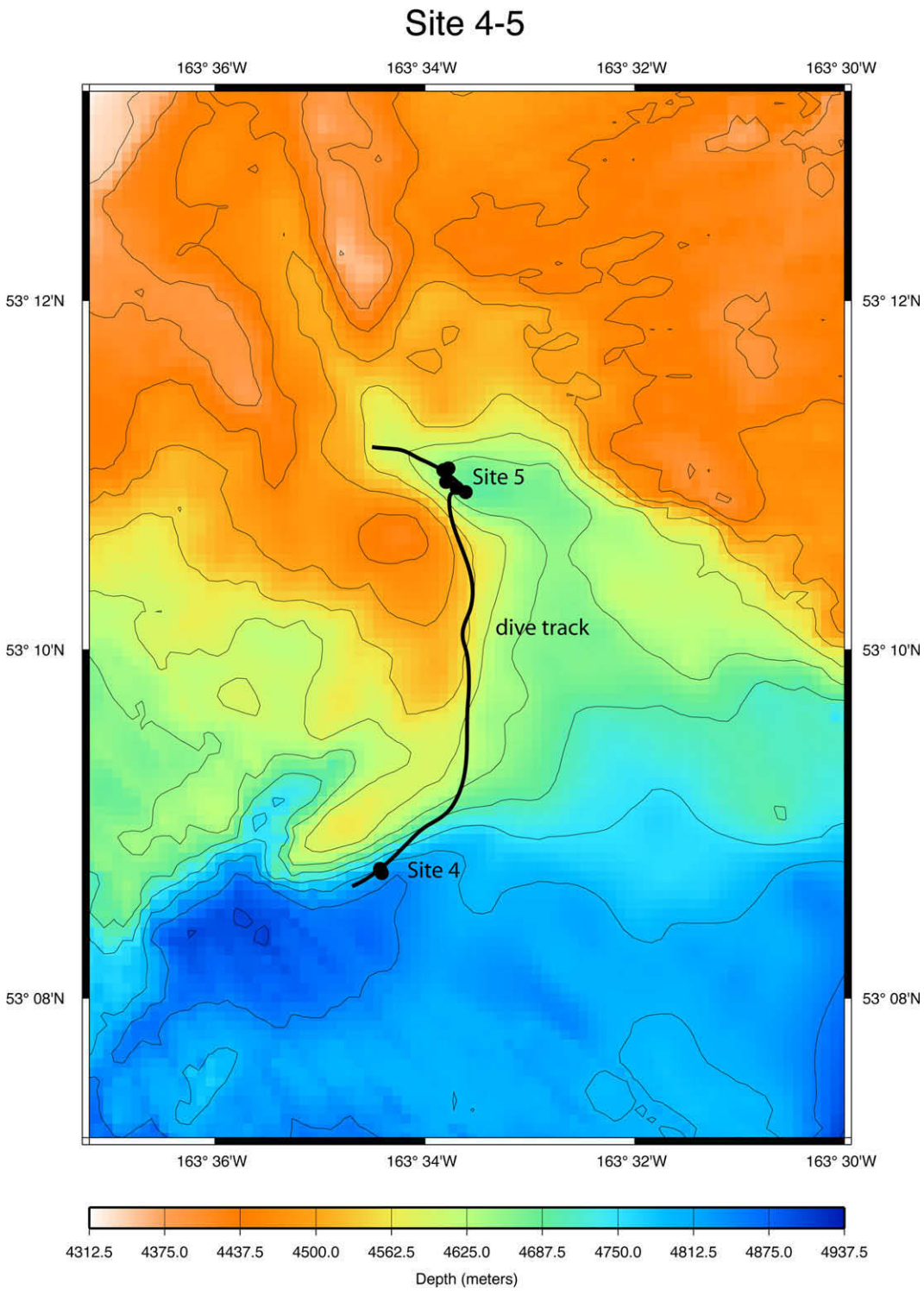

Fig. 1e. Detailed bathymetry and dive track of Sites 4 and 5.

The cores were brought to the ship's cold room immediately after recovery and microprofiles of oxygen, sulfide and pH were performed in intact cores at *in-situ* temperatures (~2 °C). The same cores were subsequently sectioned in 1 cm intervals and sub-sampled for further geochemical, foraminiferal and microbiological analyses.

3.5.1. Microsensor measurements

Microprofiles of hydrogen sulfide (H_2S) and oxygen concentrations were generated using amperometric microsensors. Measurements were performed immediately after retrieval of push cores in the cold room at *in-situ* temperature (~2 °C). The oxygen sensor was a Clark-type microelectrode with a built-in reference and a guard cathode (Jørgensen and Revsbech, 1985; Revsbech and Jørgensen, 1986; Revsbech,1989). The electrodes had a sensing tip of 20–40 μm, a stirring sensitivity of <2% and a 90% response time ⩽1 s. H_2S microgradients were measured using miniaturized amperometric sensors with an internal reference and a guard anode (Jeroschewsky et al., 1996). The sensors had a tip diameter of 40–60 μm. For vertical profiling, the sensors were attached to a

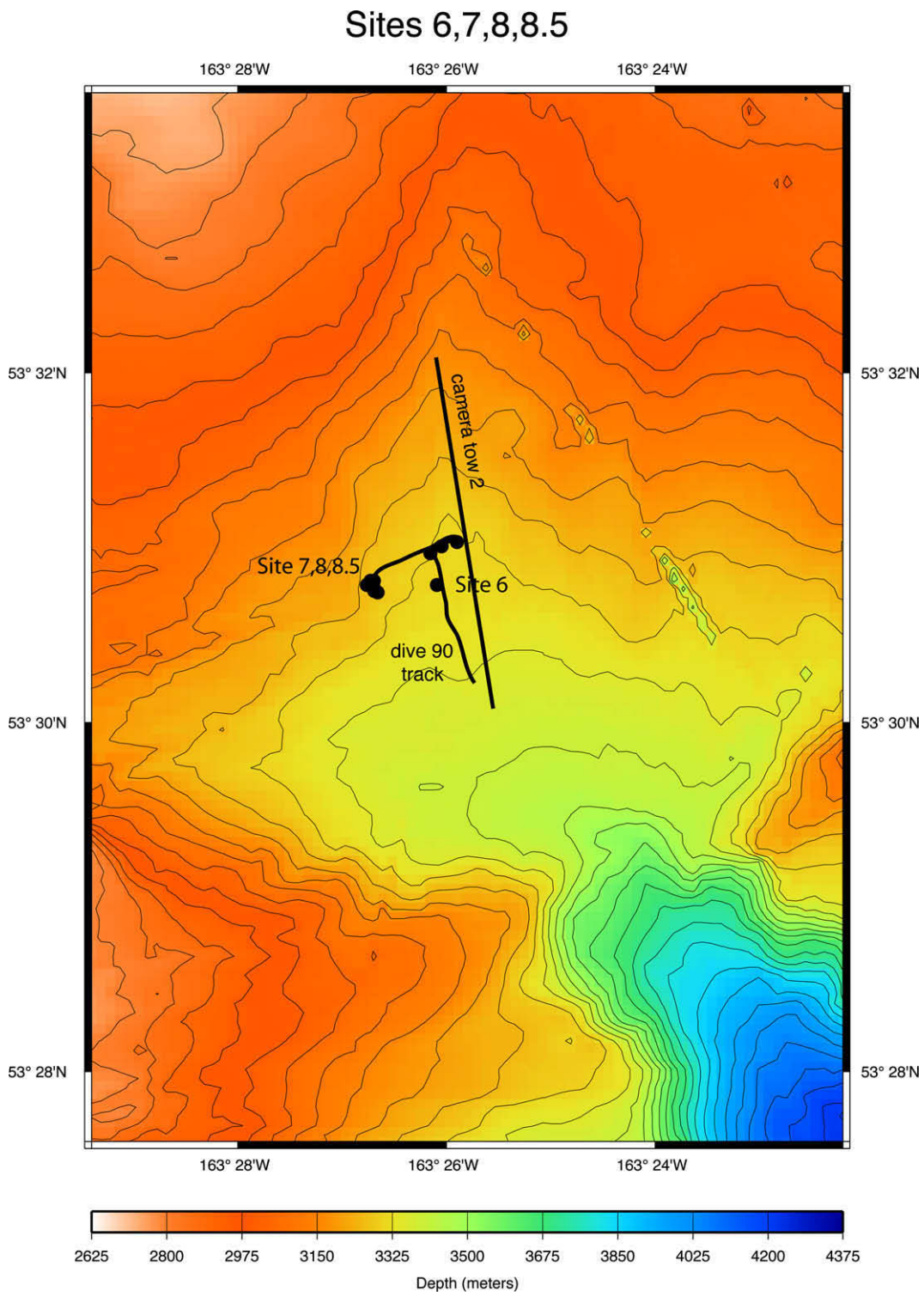

Fig. 1f. Detailed bathymetry, dive track and camera tow 2 for Sites 6–8.5.

micromanipulator mounted on a heavy stand. Signals were amplified by a picoammeter (Unisense PA 2000) and data were recorded directly on a computer. Parallel to the sulfide profiles, pH values were measured using a long needle combination pH electrode (Diamond General) connected to a high-impedance mV-meter. The values were used to calculate the total sulfide concentrations. Measurements were performed in vertical increments of 250 μm for oxygen and 1 mm for H_2S and pH.

3.5.2. Porewater chemistry

Cores were sectioned in 1 cm intervals and placed in centrifuge tubes in a nitrogen atmosphere utilizing a glove box, and pore fluids were extracted by centrifugation. Porewaters were extracted from cores taken in different habitats. The methods utilized for the determination of alkalinity, dissolved sulfate and dissolved ammonium have been described by Gieskes et al. (1991). We chose to measure alkalinity, dissolved sulfate and dissolved ammonium

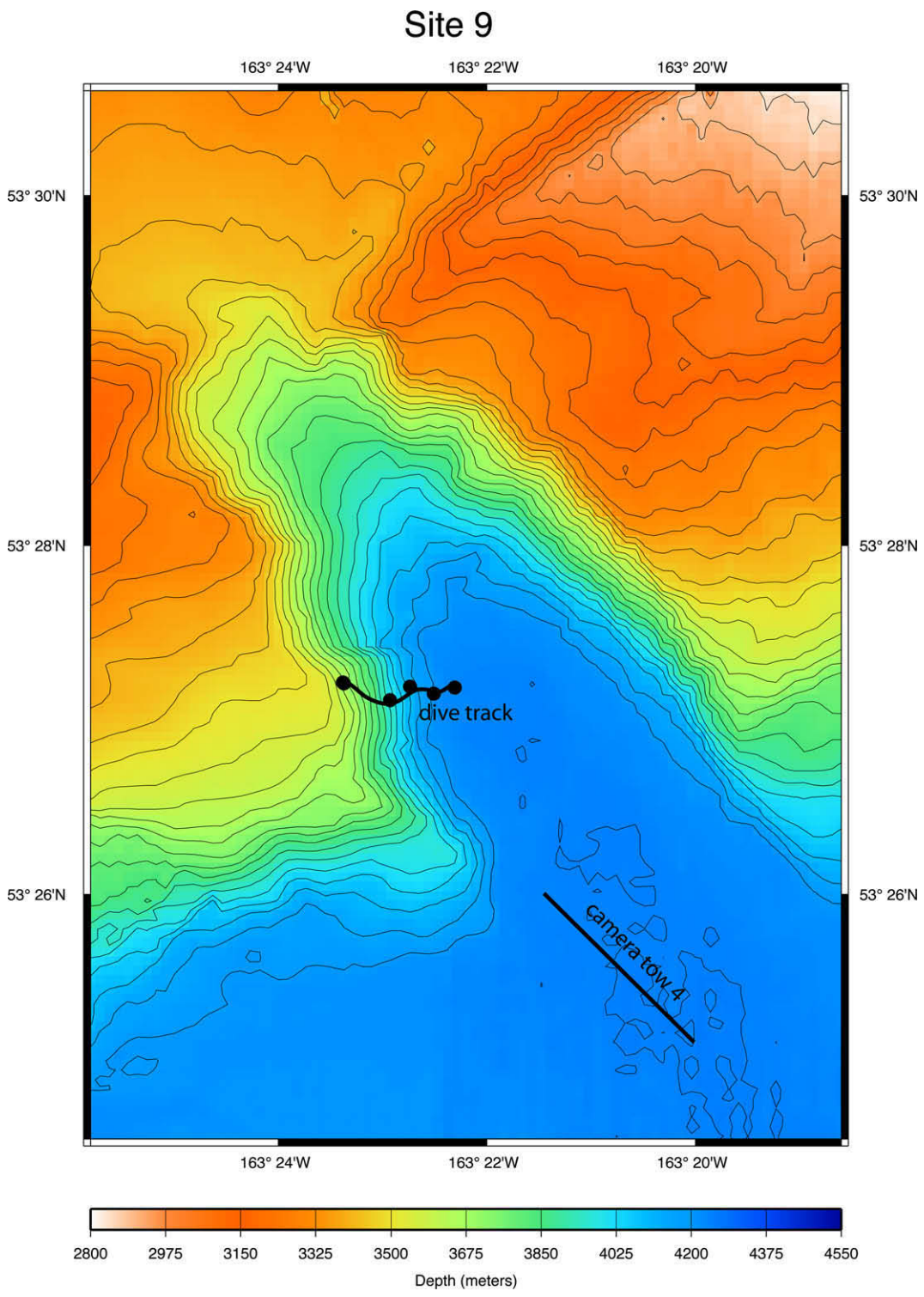

Fig. 1g. Detailed bathymetry, dive track and camera tow 4 of Site 9.

because sulfate reduction is accompanied by increases in alkalinity and ammonium, which can be expected by processes that involve the biochemical oxidation of nitrogenous marine organic matter. The isotopic and chemical compositions of the authigenic carbonates were analyzed using the same methodologies described by Gieskes et al. (2005). For each dive, whenever possible, cores for porewater geochemical analyses were taken adjacent to cores used for faunal analyses. Two cores were collected in similar environments at Site 3 in dives 88 and 89 (88-8 (1964 m) and 88-14 (1988 m). For dive 89, core 89-20 (4822 m) was collected at Site 4, and core 89-27 (4620 m) was collected at Site 5. During dive 90, core 90-8 (3310 m) was collected at Site 6, and core 90-32 (3268 m) was collected at the edge of a clam bed (Site 7). Core 91-42 (3280 m) was collected in a separate clam bed (Site 8.5), while core 91-21 (3284 m) was collected in the pogonophoran field (Site 8).

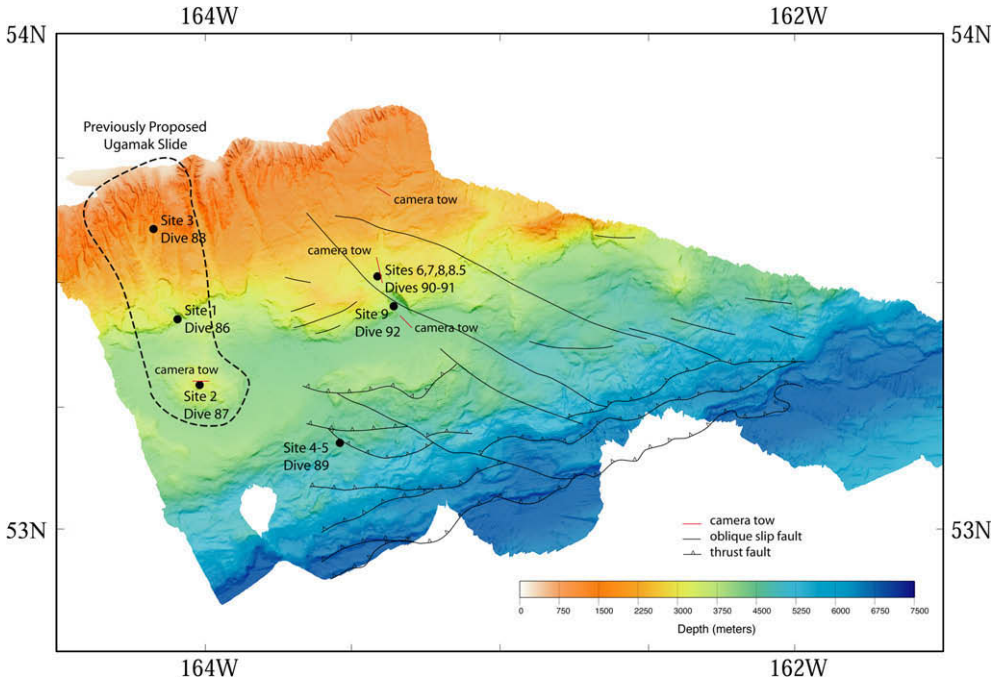

Fig. 1h. Bathymetry and structural interpretation of the region. Previously proposed Ugamak Slide is indicated as are the Sites described in the text. Structural interpretation is from Lewis et al. (1988). The lack of interpretation in the western region is due to an absence of available sub-bottom imaging.

Table 1
Sampling stations and positions.

Site	Jason dive	Date	Habitat	Depth (m)	Latitude (N)	Longitude (W)
1	86	11-Jul-04	Canyon mouth	3600	53°25.588	164°7.363
2	87	12-Jul-04	Mid-basin block	3190	53°17.476	164°2.773
3	88	13-Jul-04	Midslope Canyon	1965	53°36.469	164°12.000
3	88	13-Jul-04	Midslope Canyon	1988	53°36.701	164°12.335
4	89	14-Jul-04	Scarp	4822	53°8.72	164°34.410
5	89	14-Jul-04	Deep canyon	4620	53°11.038	164°33.772
6	90	15-Jul-04	Flat slope	3310	53°30.786	164°26.087
7	90/91	15-Jul-04	Seep/clam bed/rock gardens	3267	53°30.809	164°26.692
8	91	18-Jul-04	Pogonophoran field	3283	53°30.775	164°26.698
8.5	91	18-Jul-04	Clam bed 2/rocks	3277	53°30.752	164°26.686
9	92	19-Jul-04	Canyon Mouth Fault	3580–4240	53°27.147	164°22.506

3.5.3. Sediment analyses

Each 1 cm section down to 10 cm of the collected sediment cores was sub-sampled for the analyses of total carbon and nitrogen content, as well as for carbon and nitrogen stable isotopic composition. The analyses of carbon and nitrogen stable isotopic composition of sediment samples were performed by M. Fogel at the Carnegie Institute in Washington, D.C. An aliquot (~400–1000 μg) of sample was weighed into a tin or silver capsule, and analyzed on a CE Instruments, NA 2500 series EA coupled to a continuous-flow, stable isotope ratio mass spectrometer (Finnigan MAT, DeltaplusXL).

At all sites, the top 0–1 cm of a sediment core was sectioned for the determination of chl *a* and TOC and kept frozen until analysis. Chloroplastic pigments (chl *a* and phaeopigments) were determined spectrophotometrically according to Plante-Cuny (1973) after extraction with 90% acetone. The sum of chl *a* and phaeopigment was operationally defined as chloroplastic pigments equivalent (CPE) and was used as a measure of input of phytodetrital material to the sediments (Pfannkuche and Soltwedel, 1998). The contribution of chl *a* to the CPE (% chl *a* in CPE) is a good indicator of "fresh" material derived from primary production. Ratios of chl *a* to TOC content (chl *a*:TOC; in μg chl *a* mg^{-1} C) were calculated, assuming a C/chl *a* conversion factor of 42.5 (Bernal et al., 1989).

3.6. Microbial counts

A sub-sample of 1 cm^3 sediment of each 1 cm section of the cores down to 10 cm was transferred to 9 cm^3 sterile-filtered sea water– formaldehyde solution (4%) and stored at 4 °C for the enumeration of stained cells (Acridine Orange Direct Counts) using an epifluorescent microscope (Meyer-Reil, 1983; Epstein and Rossel, 1995). Additional samples for the analysis of microbial diversity and activity were taken from the same sub-samples, and results are reported elsewhere (Ziebis and Haese, 2005; Ziebis et al., 2005b; Ziebis et al., unpublished; Hewson et al., unpublished).

3.7. Macrofauna

At most stations, 3–5 cores per site were sectioned vertically at 0–1, 1–2, 2–3, 3–5, 5–10 and 10–15 cm intervals. Sections from the top 5 cm were preserved in 8% buffered formalin without sieving. The formalin solution was obtained by diluting 37% formaldehyde

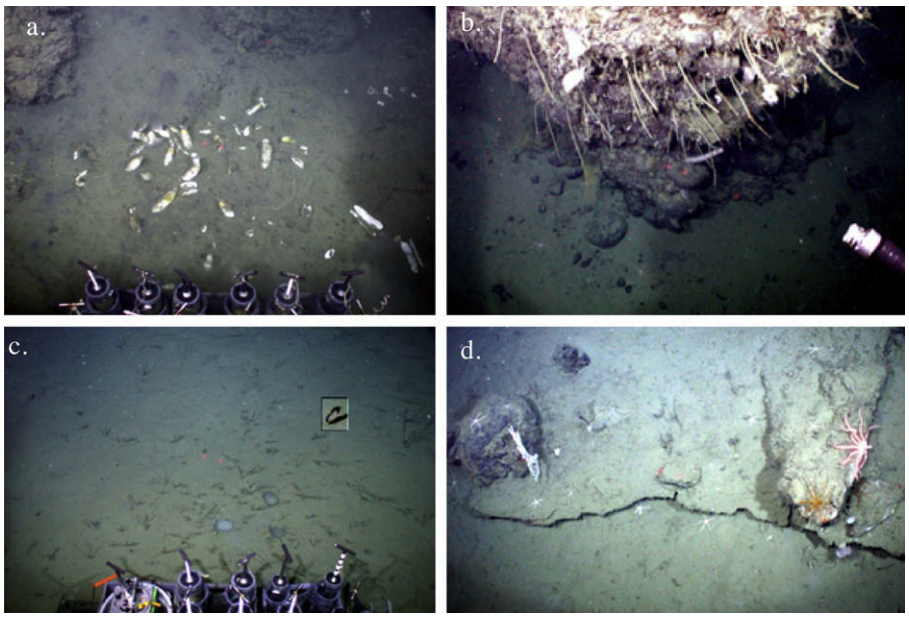

Fig. 2. Unimak habitats. (a) *Vesicomya extenta* Clambed (3267 m); (b) Weeping Rock; (c) pogonophoran field; (*Siphonbrachia*); (d) Rock away from Seeps. For scale, in each of the images the two red dots (laser pointers) are about 10 cm apart.

by a ratio of 8:2 with filtered seawater and buffering with borax. The bottom two fractions were sieved through a 0.3 mm mesh prior to preservation. In the laboratory all macrofaunal samples were resieved through a 0.3 mm mesh, sorted under a dissecting microscope at 12× magnification and identified to the lowest taxonomic level possible. Scoop bag sediments (1–2 scoops per station) were sieved live with filtered seawater through a 0.3 mm mesh and invertebrates were sorted and identified to the extent possible under a dissecting microscope at sea. Animals were allowed to clear guts overnight, then specimens were either frozen (−80 °C) in preweighed tin capsules ("boats") or combusted vials for subsequent stable isotope analysis or preserved in 8% formalin to generate reference specimens for later species-level identification. A number of epifaunal animals were removed from rocks for isotope analysis by ROV manipulator and placed in a biobox for return to the surface. These were frozen at -80 °C and returned to the laboratory.

Metazoan stable isotope samples were powdered (if large) and acidified with 1% $PtCl_2$ to remove inorganic carbon. Analyses were performed on an Europa ANCA-GSL CN analyzer (PDZ Europa Ltd., Sandbach, UK) coupled to a PDZ Europa 20-20 mass spectrophotometer at the UC Davis Stable Isotope Facility. Isotope ratios are expressed as $\delta^{13}C$ or $\delta^{15}N$ in units of per mil (‰), with standards as described in Levin and Mendoza (2007).

3.8. Foraminifera

Each core designated for foraminiferal analyses was vertically sectioned and preserved in 4% formaldehyde buffered with at least a tablespoon of borax. A 4% formaldehyde solution was obtained by diluting 37% formaldehyde by a factor of 10 with filtered seawater. The resulting solution has previously been reported as 4% formalin, while others have reported this as 10% formalin. Four cores were examined for this study, two from a seep environment (Site 8) and two from non-seep environments (Sites 3 and 6). Cores were sectioned as follows: 0–1 cm; 0.5 cm intervals from 1 to 3 cm, then 1 cm intervals to at least 10 cm. In the laboratory, 65 ml of a rose Bengal stain solution (1 g L^{-1} of 4% buffered formaldehyde) was added to each section and allowed to stain for at least 1 week. Samples were wet-sieved using 150 and 63 μm mesh sieves, and specimens in the >150 μm fraction were wet-picked, sorted onto micropaleontological slides and identified. Soft-walled taxa were not included in the analyses. Only specimens with at least one chamber stained red were considered as living or recently living at the time of collection. These procedures are the same as those followed by Rathburn and Corliss (1994), McCorkle et al. (1990, 1997), and Rathburn et al. (2003), among others. Since rose Bengal stains protoplasm, dead specimens that still contain protoplasm could be counted as living (Bernhard, 2000; Bernhard et al., 2006). However, a conservative approach when using rose Bengal can provide reasonable estimates of the living population (Murray and Bowser, 2000).

4. Results

4.1. Ugamak Slide

Here, we present limited geological results to characterize the nature of environmental conditions in the study area. A more detailed discussion of geological results will be presented elsewhere. Analyses of our multibeam survey data showed that the feature in the study area identified from previous GLORIA images as the "Ugamak Slide" by Fryer et al. (2004) is not a slide that might have been associated with the 1946 earthquake and tsunami (Fryer and Tryon, 2005). The ~10-km-wide region of the proposed slide scar is characterized by a high density of deeply incised submarine canyons that are indistinguishable from those of adjacent slopes for many 10 s of km, a morphology that would have taken much longer to develop than 60 yrs (Fig. 1a). The slope terminates at about 3500 m in what appears to be a steep fault-controlled escarpment. What was speculated to be the toe of the slide (Site 2) has the morphology of an isolated, 20-km-wide, 800 m-high, fault-bounded block located within the main Aleutian Terrace basin. Numerous NW–SE striking escarpments can be seen in the bathymetry that are comparable to those seen and described all along this margin (Lewis et al., 1988), features that would not be easily preserved in a slide toe. This, combined with the isolation of the block feature, the maturity of the adjacent slope, and the absence of slide

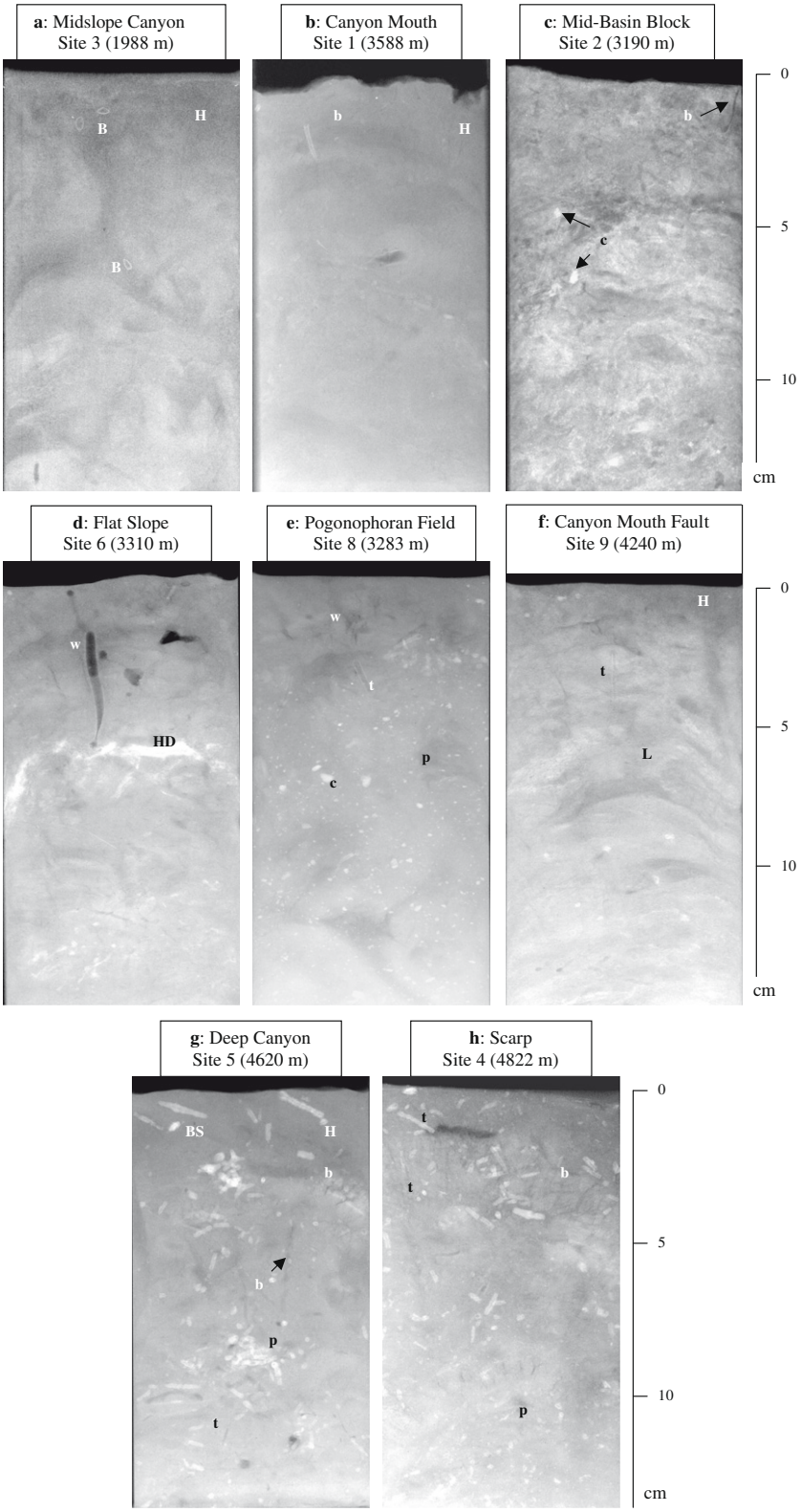

Fig. 3. X-ray images of the sediment structure at the sites explored during the Unimak cruise in July 2004. (a) Midslope Canyon (Site 3, 1988 m); (b) Canyon Mouth (Site 1, 3588 m); (c) Mid-basin block (Site 2, 3190 m); (d) Flat Slope (Site 6, 3310 m); (e) pogonophoran field (Site 8, 3283 m); (f) Canyon Mouth Fault (Site 9, 4240 m); (g) deep canyon (Site 5, 4620 m); (h) Scarp (Site 4, 4822 m). Key features are shown: homogenized sediment (H), high density sediment (HD), laminations (L), bivalves (B), bivalve shell remains (BS), concretions (c), pebbles (p), tubes (t), burrows (b), worms (w). Scale in centimeter is indicated on the right. Some of the sediment slabs used for X-ray images were also photographed (see Fig. 7).

debris adjacent to the block, indicate that this feature did not result from a slide associated with the 1946 earthquake but is more likely an uplifted, fault-bounded, basement high. The lack of seismic imaging of the region prohibits a more thorough analysis.

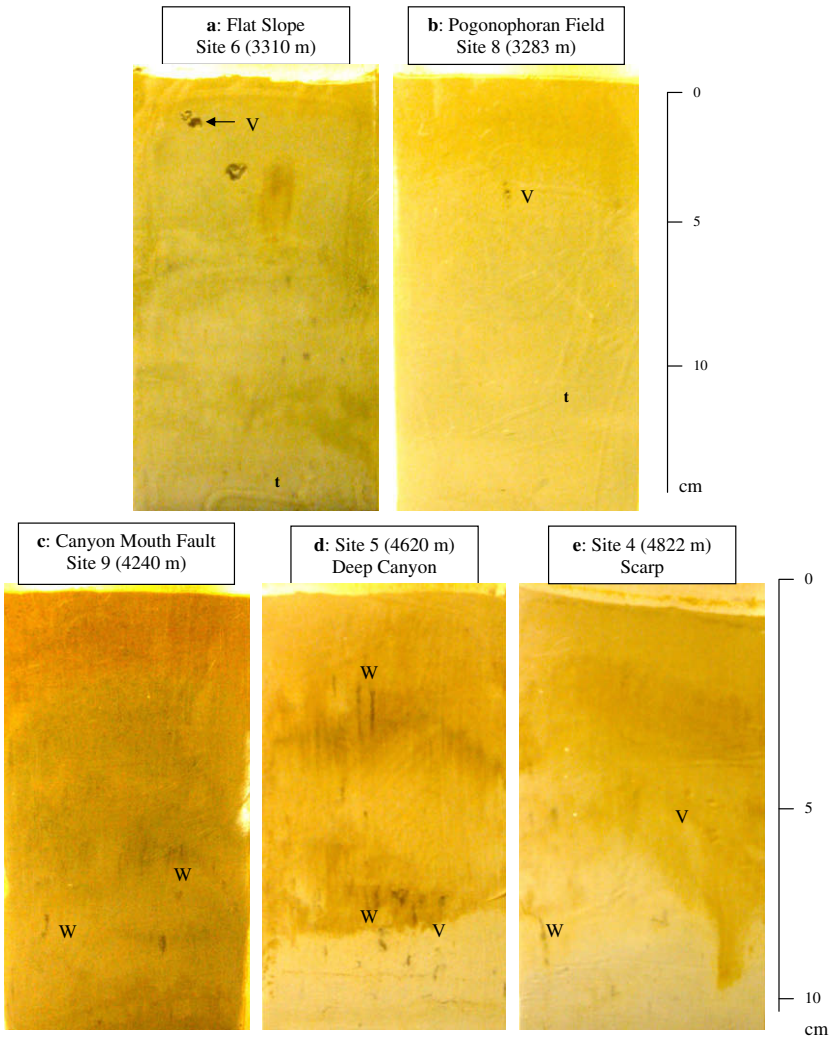

Fig. 4. Digital images of sediment from five selected sites explored off Unimak (Alaska), showing sediment profile texture, gradient of bulk density, through color change and biogenic structures. These photographs were taken from the same slabs used for X-radiographs of Fig. 6. Key features are shown: Active feeding voids (V), worms (W) and tube fragments (t). Scale in centimeter is indicated on the right.

4.2. Site descriptions

The following site descriptions are based primarily on bathymetric mapping, visual evidence from ROV-mounted cameras, and from shipboard observations of sediments. Site locations are presented in Fig. 1a–h and images of habitats are included in Figs. 2a–d, 3a–h and 4a–e.

4.2.1. Site 1 – Canyon mouth at midslope terminal escarpment (3588 m)

Dive 86 (Fig.1a and b) targeted the intersection of the major midslope basin and the landward bounding escarpment at ~3588 m depth where a relatively short, steep-sided indentation in the escarpment had formed that may be indicative of a relatively recent slope failure. A northerly transect along the base of the west wall near the mouth of the scar revealed a steep escarpment consisting of a series of vertical steps of horizontally bedded mudstone with a basal debris field of angular blocks. This area has a relatively muddy bottom with evidence of current scouring. X-radiographs of sediment appear homogeneous, and few biological structures are evident (Fig. 3b). Dominant epibenthic taxa visible from the ROV cameras included Cnidaria (sea pens, anemones), Echinodermata (brittle stars), Porifera (stalked sponges) and xenophyophores. Cnidaria (actinarians and pennatulids) were observed on rocky outcrops. Common taxa on outcrops included gorgonians (sea fan), Porifera (tulip sponges), Cnidaria (antipatharians) and Echinodermata (crinoids). Echinodermata (brittle stars) reached high densities on sediment terraces.

4.2.2. Site 2 – summit of faulted Mid-basin Block (3190 m)

Dive 87 (Fig. 1a and c) occurred at the 3190 m summit of a large, roughly circular bathymetric high, elevated ~800 m above the center of the major midslope basin. This feature exhibits a series of NW striking escarpments that may be due to right-lateral faulting as observed throughout the survey area and noted in the eastern half of the area (Lewis et al., 1988). The summit region is sediment covered and featureless. However, as we transected downslope to the south we encountered a small vertical escarpment probably associated with the strikeslip faulting. The summit of the mid-basin block was characterized by bioturbated but compacted sediments, though variations in density in X-radiographed sediments indicated that mud rip-up clasts were present (Fig. 3e). This suggests that sediments were redeposited, probably by turbidity currents, and possibly bioturbated by macrofauna. The mid-basin block had the highest proportional abundance of fish (Chordates; Table 2).

Table 2
Environmental and megafaunal characteristics of Tow Cam survey sites along the Aleutian margin. Megafaunal densities are broken down by phyla and presented with ±1 SE. Unlike letters represent significant ($p < 0.05$) differences among sites using SNK post hoc tests where ANOVA indicated a significant site effect. The transect for Camera Tow 1 is shown in detail in Fig. 1c; Camera Tow 2 transect is shown in detail in Fig. 1f; Camera Tow 3 transect is only shown in Fig. 1a; Camera Tow 4 transect is shown in detail in Fig. 1g.

Tow #	001	002	003	004
Feature traversed	Mid-basin block	Slope	Slope	Abyssal terrace basin
Date (tow start)	July 12 2004	July 16 2004	July 16 2004	July 19 2004
Start latitude	53.17.8995	53.30.0458	53.40.7684	53.25.0000
Start longitude	164.04.0006	163.25.6481	163.22.4380	163.19.9980
Stop latitude	53.17.8995	53.32.0867	53.41.4281	53.26.0141
Stop longitude	164.00.7294	163.26.1127	163.23.5618	163.21.4541
Transect length (m)	10150	9800	9000	7200
Depth range (m)	3348–3162	3378–3168	2016–1904	4238–4235
Bottom photos	1750	1800	1800	1200
Photos analyzed	153	105	130	120
Bottom type	Soft sediment	88% Soft sediment – 12% outcrop mix	Soft sediment	Soft sediment
T (°C)	1.49	1.47	1.96	1.49
Salinity	34.67	34.67	34.57	34.69
Oxygen (μM)	121.43	112.05	49.55	134.82
Mean phot area (m^2)	15.00	19.16	12.45	17.35
Bottom surveyed (m^2)	2250.30	2011.80	1245.62	2080.83
Total megafauna (# m^{-2})	0.3180 ± 0.0170 A	0.4320 ± 0.029 A	5.3800 ± 0.4270 B	0.2650 ± 0.0110 A
Porifera (# m^{-2})	0.0004 ± 0.0004 A	0.0200 ± 0.0040 B	0.0100 ± 0.0040 C	0.0210 ± 0.0030 B
Cnidaria (# m^{-2})	0.0470 ± 0.0050 A	0.0470 ± 0.005 A	0.4020 ± 0.0350 B	0.0730 ± 0.0060 A
Echiura (# m^{-2})	0 ± 0A	0.0004 ± 0.0004 A	0.0060 ± 0.0020 B	0 ± 0A
Arthropoda (# m^{-2})	0.0050 ± 0.0020 A	0.0040 ± 0.001 A	0.0370 ± 0.0080 B	0.0020 ± 0.0010 A
Mollusca (# m^{-2})	0.0020 ± 0.0020 A	0.0010 ± 0.0010 A	0.0160 ± 0.0040 B	0.0010 ± 0.0010 A
Echinodermata (# m^{-2})	0.2290 ± 0.0140 A	0.3530 ± 0.0270 A	4.8890 ± 0.4070 B	0.1480 ± 0.0090 A
Hemichordata (# m^{-2})	0 ± 0A	0 ± 0A	0 ± 0A	0.0050 ± 0.0020 B
Chordata (# m^{-2})	0.0350 ± 0.0040 A	0.0060 ± 0.0020 B	0.0190 ± 0.0040 C	0.0150 ± 0.0030 BC
Lebensspuren (# m^{-2})	0.9120 ± 0.0540 A	3.8890 ± 0.2700 B	16.4200 ± 1.2720 C	5.3630 ± 0.2590 B

4.2.3. Site 3 – Midslope Canyon (1965–1988 m)

Dive 88 (Fig. 1a and d) was located within a deeply eroded canyon along the midslope at a depth of ~1975 m. A transect across and up the canyon revealed featureless sediment except for a small area of mixed and somewhat rounded boulders that were composed of rocks varying from mudstones to coarse conglomerates, probably transported down the canyon. Sediments collected at this site were fine grained, relatively homogeneous and soupy with appreciable bioturbation. Several small bivalves were visible in one X-ray (Fig. 3a). Tubes of the foraminiferan *Bathysiphon* sp. were common and readily visible rising from the sediment–water interface. Bottom images revealed abundant pits and mounds observed on the surface. Echinodermata (asteroids and brittle stars) were abundant.

4.2.4. Site 4 – scarp and Site 5 – Deep Canyon (4620 m)

Dive 89 (Fig. 1a and e), at a depth of 4500–4822 m, surveyed a canyon cutting through the upper portion of the stepped lower slope thrust region. The canyon marked the intersection of two mapped thrust faults. A large number of disturbance-related seafloor features were found distributed throughout the area, including both up- and downslope-facing escarpments of less than 1 m, extensional fractures, seemingly randomly oriented rock outcrops and rock and boulder debris. Most prominent among these features was an E-W-oriented fracture with vertical sides and fresh, sharp upper edges in horizontally bedded sediments that was up to 2 m wide and 1 m deep. An additional E-W striking short and fresh escarpment was found 20 m upslope with an offset down to the south. The scarp (Site 4) exhibited fine, dark colored sediment. High densities of Echinodermata (brittle stars and holothurians) were observed. Infaunal observations were not conducted on board. The canyon floor (Site 5) had relatively fine sediments at the surface, and X-radiographs showed high-density features that included gravel, carbonate pebbles and animal structures within the sediments (Fig. 3g and h). These appeared in clusters throughout the core. An *Acharax* shell and empty pogonophoran tubes were recovered from the scoop bag, suggesting possible recent seep activity in the area.

4.2.5. Site 6 – Flat Slope (3310 m)

Dive 90 (Fig. 1a and f) sampled a site located above the head of a very large steep-sided scar in the landward wall of the midslope basin where a major right-lateral strikeslip fault crosses the margin (Lewis et al., 1988). The area has an inverted fan morphology indicative of downslope sediment flow into the scar, similar to that often found upslope of the headwall of slumps or canyons. This site was characterized by fine sediment with a relatively high density of epibenthos, dominated by Echinodermata (urchins and ophiuroids; Table 2). Based on Tow Cam images, the slope at 3200 was approximately 88% soft-sediment bottom, while rocky outcrops covered 12% of the seafloor. An X-radiograph of sediments from this site showed a worm tube extending downcore to a high-density layer about 8–10 cm below the surface (Fig. 3d). Otherwise sediments appeared bioturbated. Sulfur bacteria (*Beggiatoa*-like) were present but sparse in scoop samples.

4.2.6. Site 7 – Seep Site (3268 m)

Dives 90 and 91 (Fig. 1a and f) sampled a site with indicators of methane/sulfide/fluid seepage. This site was about 3 km to the east of Site 6, located at an outcrop which extends ~200 m along strike of the fault and steps up to the SW. Rock exposures varied from poorly lithified mudstone to a poorly lithified conglomerate with mudstone clasts. Surface sediments were capped in places with a thin pavement that was often undercut at its downslope edge. Three seep habitats are described in the seep area: clam beds, rock gardens and pogonophoran fields.

4.2.6.1. Clam beds. Small patches of vesicomyid clams and pogonophorans were observed at 3267–3284 m, on the upper and lower zones of a 15 m-high rock ledge. One patch (about 1.5 × 2 m) was comprised mainly of *Vesicomya extenta* and *Vesicomya diagonalis* (identifications by E. Krylova, Shirshov Institute of

Oceanology, Nakhimovskii Prospect, 36, Moscow 117851, Russia. Identifications made in September 2005) (Fig. 2a). Many of the *Vesicomya* had 1 or more large anemones on the upper portion of the valves. A second patch (<0.5 m across) had *V. diagonalis*. Both living and dead shells were present in the smaller patch. Some of the sediment surrounding the clams was black, suggesting the presence of sulfide. Large pogonophoran tubes (species unidentified) were present in a zone between the vesicomyids and the rock ledge (upper region, 3267 m). Scoop bag collections from the clam beds contained mainly gravel with small amounts of mud. Yellow and white sulfur bacteria were abundant and large (retained on a 0.3 mm mesh). These are filamentous, *Beggiatoa*-like sulfide oxidizing bacteria. No genetic work was done to determine if they were actually *Beggiatoa*.

A species of the polychaete *Capitella* was observed living on the lip of the smaller vesicomyid, *V. diagonalis*, with tubes etched into the shell. Up to 10 or more individuals were present on some clams. Most *Capitella* had eggs present at the time of recovery.

At a second clam bed sampling area, *V. extenta* were found living partially on conglomerate rock with only a few centimeters of sediment covering the rock in places. They appeared to have hauled themselves on to the rocks. A small solemyid was recovered from deep in one of the tube cores at the clam bed edge.

4.2.6.2. Rock Gardens (rocks covered with organisms). The rocks close to the clam beds were a mixture of mudstone and conglomerate, with carbonate plates present in some places. Rocks were heavily colonized in the vicinity of the seep, with feathery hydroids, anemones, serpulid polychaetes and some corals present. On one rock – referred to as 'Weeping Rock', all organisms were growing down towards the base (Fig. 2b). Faunal samples were collected to look for evidence of incorporation of methane-derived carbon in organic carbon isotope signatures.

4.2.7. Site 8 – Pogonophoran Field (3283 m)

A third seep habitat type, comprised of tufts of pogonophorans (*Siphonobrachia* sp.) was observed about 10 m from the rock ledge (Fig. 2c). Sediments were fine grained, soft and deep (Fig. 4b). X-radiographs showed small, high-density structures (gravel or carbonates) throughout the core (Fig. 3e). The upper few centimeters were highly bioturbated with burrows visible. Pogonophoran densities were 10–20 m^{-2}. Measured pogonophoran tubes ranged from 22 to 36 cm length (1 mm diameter), with over half of the tube forming a root like structure below ground. At least one was gravid and released both unfertilized eggs and fertilized embryos (which did not develop). Pogonophoran tubes were colonized by a variety of protozoans and invertebrates and appeared fuzzy, due to growth of protists and tube-building polychaetes. Subsequent collection suggested the heavily colonized tubes did not contain living pogonophorans. The most common epizoonts were *Cibicides wuellerstorfi* (a calcareous, epifaunal foraminiferan), a branched astrorhizinid, and two species of ampharetid polychaetes. Also observed were hydroids, corals, an unidentified egg case, white polyps, a barnacle and an isopod.

4.2.8. Site 9 – Canyon Mouth Fault scarp at midslope terminal escarpment (3580–4240 m)

Dive 92 (Fig. 1a and g) explored a transect westward across the floor of the scar below the dive 90–91 site and up the western wall covering a depth range of 3580–4240 m. The floor was sediment covered and featureless with increasing amounts of rock debris approaching the wall. The ~700 m wall consisted of a ~45° slope of highly fractured mudstone that had undergone a large degree of brittle deformation, i.e., it appeared that this was within the deformation zone of the major right-lateral strikeslip fault (Lewis et al., 1988). Floor sediments were very fine indicating little current. Mottled sediments of various densities were shown in X-radiographs (Fig. 3f). Burrows were present in the upper 3–4 cm but few biogenic structures were evident deeper in the sediments. Infauna were sparse and were dominated by agglutinated protozoans; infaunal xenophyophores were common. Corals were collected from the wall.

4.3. Findings

4.3.1. Sediment characteristics

Total organic carbon (TOC) and total nitrogen (TN) in surface sediments ranged from low values of 0.42% and 0.05%, respectively, at the Mid-basin Block (Site 2) to a high of about 2.2% and 0.27%, respectively, in the scarp (Site 4) and Midslope Canyon (1988 m; Site 3) (Table 3). The C:N molar ratios were relatively low and did not show major changes, varying between 7.79 and 8.89, suggesting high quality of the sedimentary organic carbon. Notably, all the canyon C:N ratios were <8.0 while all the other sites were >8.0 (Table 3). The bulk of photosynthetically produced organic matter exported from the photic zone usually reaches the sea bottom in the form of detritus particles and is the main food source for deep-sea benthos (Pfannkuche, 1993). Sedimentary chl *a* concentrations denote fresh algal input. The CPE content in surface sediments (Table 3) was correlated with sediment C and N contents, ranging from 0.72 μg g^{-1} at the Mid-basin block (Site 2) to a high of 34.40 μg g^{-1} in the Midslope Canyon (Site 3) and the terrace

Table 3
Sediment organic chemistry of the top 1 cm of the nine sites explored during the UNIMAK cruise. Only %C, %N and $\delta^{13}C$ and $\delta^{15}N$ measurements were made for 1988 m samples at Site 3.

Site		% C	% N	C/N	$\delta^{13}C$ (‰)	$\delta^{15}N$ (‰)	chl *a* (μg g^{-1} DW)	Phaeop (μg g^{-1} DW)	CPE (μg g^{-1} DW)	chl *a* in CPE (%)	chl *a*:TOC ratio (μg mg C^{-1})
1	Canyon mouth (3588 m)	1.49	0.19	7.84	−21.11	7.82	3.57	9.05	12.62	28.26	13.49
2	Mid-Basin Block (3190 m)	0.42	0.05	8.40	−21.48	12.85	0.15	0.57	0.72	20.80	2.17
3	Midslope Canyon (1965 m)	1.35	0.17	7.94	−20.64	7.12	8.51	25.89	34.40	24.70	23.85
3	Midslope Canyon (1988 m)	2.11	0.27	7.81	−20.43	7.22					
4	Scarp (4822 m)	2.2	0.27	8.15	−21.65	9.72	2.76	1.75	4.51	61.19	13.68
5	Deep canyon (4620 m)	1.09	0.14	7.79	−23	10.09	1.81	2.48	4.29	42.19	9.43
6	Flat Slope (3310 m)	1.28	0.16	8.0	−21.70	3.79	2.45	6.61	9.06	27.04	8.13
7	Seep site (3268 m)	1.24	0.15	8.27	−22.34	0.61	0.16	3.75	3.91	4.09	0.84
8	Pogonophoran field (3284 m)	1.69	0.19	8.89	−22.8	3.22	3.58	6.32	9.90	36.16	12.15
9	Canyon Mouth Fault (4240 m)	1.41	0.17	8.29	−22.14	4.74	8.00	22.23	30.23	26.46	26.23

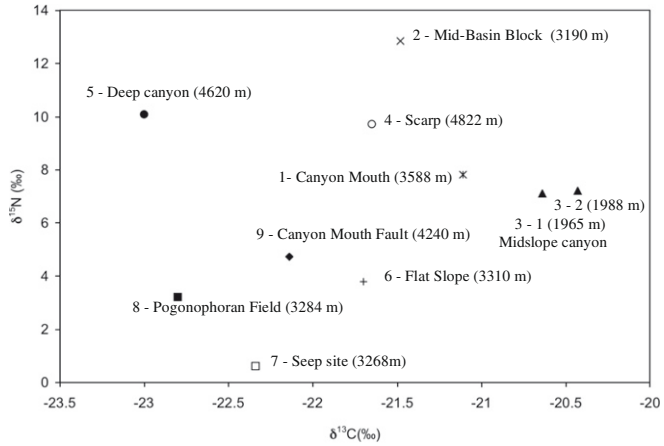

Figure 5. Dual isotope plot of $\delta^{15}N$ and $\delta^{13}C$ analyzed in surface sediments (top 1 cm).

of the Canyon Mouth Fault (Site 9). At the time of our dive, sediments of the midslope terminal escarpment were very fine, indicating little water motion and hence little horizontal transport, favoring phytoplankton settlement. Chloroplastic pigments in general were dominated by phaeopigments, which accounted for more than 70% of CPE. At Site 7 (clam beds), 96% of CPE was degraded chl *a* (i.e., phaeopigments). At Site 4 (Scarp), in spite of the low CPE concentration, 61% of it was fresh chl *a*. The chl *a*: TOC ratio, an indicator of organic matter quality (Boon and Duineveld, 1996), was lowest at Sites 2 (Mid-basin block) and 7 (clam beds), and highest at Sites 9 (Canyon Mouth Fault) and 3 (Midslope Canyon) (Table 3).

The dual isotope plot of $\delta^{15}N$ and $\delta^{13}C$ values analyzed for the surface sediments (top 1 cm) showed distinct differences among sites and with clear clustering of values at similar sites (Fig. 5). The pogonophoran field (Site 8; 3283 m) and the clam bed site (Site 7; 3268 m) showed comparably lighter C and N isotopic signatures than the other sites, evidencing the occurrence of chemosynthetically fixed carbon within sediments (Table 3, Fig. 5). In contrast, the sediment at the summit of the faulted Mid-basin block (Site 2) showed the heaviest $\delta^{15}N$ signature. The sediment at the two stations in the Midslope Canyon (Site 3) exhibited an isotopic composition (mean $\delta^{13}C = -20.5‰$; mean $\delta^{15}N = 7‰$) indicative of the input of fresh photosynthetically produced material. This site also exhibited the highest content of chl *a* and phaeopigments (Table 3).

4.3.2. Abundances of microbial cells

Highest microbe abundances were found in the sediment of the shallowest station (Site 3, Midslope Canyon, 1988 m; Fig. 6) and corresponded to the highest percentage of carbon in the surface sediment. In contrast, the lowest counts were found in the sediment samples at Site 2, on the summit of the faulted mid-basin block, where the carbon content was lowest. Thus, there was a significant positive relationship between sediment % carbon content and surface (0–5 cm; Fig. 7 shows top 5 cm integrated) microbial abundance (Fig. 7; $r^2 = 0.60$; $P = 0.065$) with almost one order of magnitude difference between sites with the highest and lowest counts. Sites with similar % C content (for example, Dive 89, Sites 4 and 5), showed very similar profiles of cell abundances (Fig. 7).

4.3.3. Sediment X-radiograph and profile photograph observations

X-radiographs (Fig. 3a–h) and digital photographs (Fig. 4a–e) of sediment slabs exhibit strong depth-related differences in sediment texture, biogenic structure, composition and gradient of bulk density. Digital photographs of the sediment column augment X-radiograph images and provide evidence of animal activity, sediment color changes and degree of consolidation. Sediments at the deeper sites shown in the digital photographs were in general very fine, soft and sticky. Worm tubes, tube fragments and active feeding void areas created by infaunal bioturbation were observed. Darker sections of the sediment in the digital color images correspond well with lighter sediment observed in the corresponding X- radiographs shown in Fig. 3.

Most of the sites show relatively homogenized sediments within the top 2 cm (Figs. 3a–h and 4a–e). The canyon sites, at 1988 m (Fig. 3a; Site 3) and 3588 m (Fig. 3b; Site 1), exhibit considerable sediment homogeneity (0–12 cm), probably caused by extensive bioturbation and/or physical mixing. Gradients in bulk density (compaction) can be seen from the change in X-ray density, with lighter and darker gray tonalities indicating higher and lower density (best represented in Fig. 3c; Site 2). Biogenic structures are few; some bivalves and tube/burrows cross the uppermost 3 cm layer. The exposed flat slope (Figs. 3d and 4a; Site 6) and isolated mid-basin block sediments at 3200–3300 m (Fig. 3c; Site 2) show more structure and sediment mottling. The flat slope at 3310 m (Figs. 3d and 4a; 3310 m; Site 6) has worms, burrows, tubes and a disturbed high density "layer" at about 6 cm deep. The mid-basin block sediments (Fig. 3c; Site 2) are a mix of consolidated and unconsolidated material with animal structures and carbonate concretions intermixed. These features suggest redeposition of sediments overprinted with bioturbation. The pogonophoran field (Fig. 3e and 4b; Site 8) at a comparable depth is more homogeneous (like the shallow canyons), but has a dense network of fine burrows in the uppermost 2 cm, abundant carbonate pebbles or concretions throughout the core, and tube fragments that probably belong to pogonophorans. The shallowest abyssal site at 4240 m (Figs. 3f and 4c; Site 9) is mottled, with few biogenic structures. There are disrupted laminations down to 11 cm. The deeper abyssal sediments at 4620 m (Figs. 3g and 4d; Site 5) and 4822 m (Fig. 3h and 4e; Site 4) exhibit extensive tube fragments present throughout the cores. These appear to be agglutinated foraminiferans (genera such as *Bathysiphon*, *Hyperammina* and *Rhabdammina abyssorum*). Burrows and void spaces are present as well.

4.3.4. Geochemical observations

Among the environmental data recorded from the Tow Cam CTD, bottom water temperature and salinity varied little among stations and transects. Oxygen levels demonstrated a marked increase with depth, confirming the presence of an oxygen minimum above 2000 m (Table 2). Tow Cam bottom water oxygen values (Table 2) are lower than the concentrations measured on board ship using oxygen microelectrodes in the overlying water of sediment cores that were retrieved from comparable areas (Fig. 8). Oxygen contamination is unlikely since sediment cores for vertical oxygen microprofiling were brought to the ship's cold room immediately upon retrieval on board the ship and microprofiles were measured at *in-situ* temperature in undisturbed cores within one hour of recovery. Tow Cam bottom water oxygen values are within 20 μM of those reported for the region by Edmond (1974). Microprofile bottom water oxygen values, with one notable exception at Site 3, also are near bottom water values for the region reported by Edmond (1974). Differences between measured concentrations may be explained by the difference in instrumentation, sensor location and sensitivity. Oxygen microelectrodes are positioned just a few millimeters above the sediment–water interface, have a very fast response time (<1 s) and a high sensitivity (nM), whereas the oxygen sensor on the Tow Cam was positioned 10 m or so above the sediment–water interface, the sensor has a slower response time, and is not as sensitive.

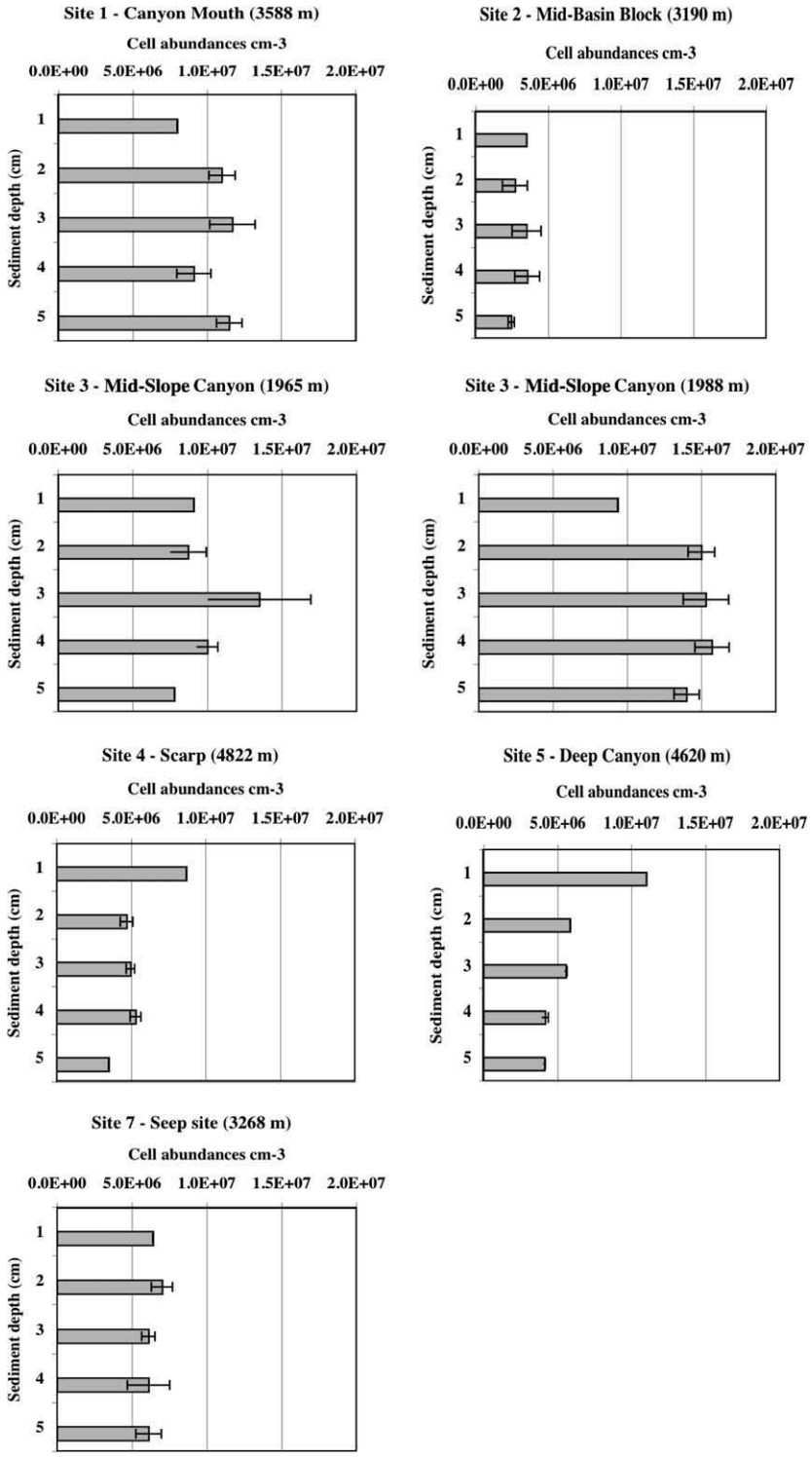

Fig. 6. Cell abundances of stained microorganisms (AODC) in the top 5 cm of collected sediment cores. Cell abundance data were not available from Sites 6, 8 and 9.

4.3.4.1. Oxygen and sulfide microprofile data. Vertical microprofiles of dissolved oxygen showed that oxygen penetration depth in the sediment column was positively correlated with water depth ($r^2 = 0.72$; $P = 0.009$) (Figs. 8 and 9). The oxic/anoxic boundary in the sediment varied from 4 mm at the relatively shallow sites (Site 3; Midslope Canyon, 1965 m) up to 20 mm or more at the deeper Sites 4, 5 and 9 (>4000 m). Thus, in contrast to the shallow stations, where only the upper most millimeters are oxic, the zone of oxygen availability at the deeper station increased to 2 cm.

At all stations, except Site 9 (4239 m), sulfide was detectable in the upper 10 cm of the sediment (Fig. 10), indicating microbial sulfate reduction occurs in the surface sediment. Concentrations were generally low, 5–15 μM. Sulfide concentrations were higher (60 μM) only at the deeper station of Site 3 (Midslope Canyon,

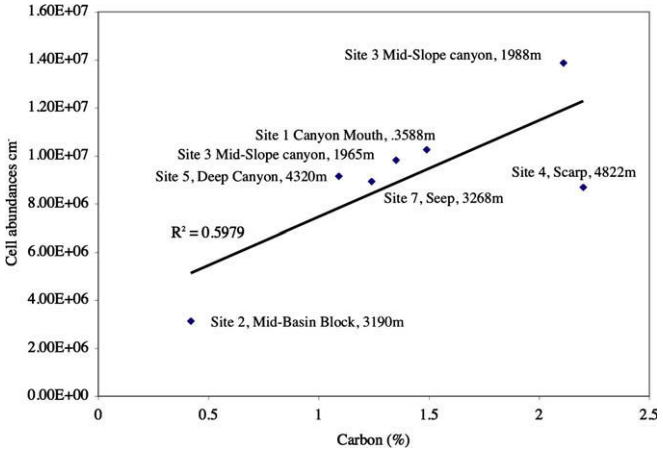

Fig. 7. Comparison of carbon content and abundances of microbial cells. Cell numbers were integrated for the top 5 cm. Cell abundance data are not available from Sites 6, 8 and 9.

1988 m), corresponding also to the highest percentage of carbon and the highest microbial cell numbers (Figs. 5 and 7).

4.3.4.2. Porewater geochemistry. Analyses of alkalinity, sulfate and ammonium (Figs. 11–13) of interstitial waters collected from a number of tube cores revealed relatively small changes down core. Most cores did not penetrate deeper than ~20 cm into the sediments and observed alkalinity changes were generally very small, though slight increases occurred with depth (Fig. 11). In addition, surprisingly small changes occurred in dissolved sulfate, even in the cores obtained in the area of pogonophorans and/or large clams encountered at Sites 7 and 8 (Fig. 12). Only Core 86-13 of Site 1, Core 88-14 of Site 3 and Core 92-27 of Site 9 (all located in areas of no apparent methane seepage) exhibited small changes in alkalinity, sulfate and ammonium (Figs. 11–13). Core 91-42 (Site 8.5) showed an appreciable increase in ammonium, which is not strongly reflected in changes in sulfate and alkalinity. Rapid depletions in porewater sulfate (resulting from anaerobic oxidation of methane coupled to sulfate reduction; e.g., Gieskes et al., 2005) were not evident in the profiles of alkalinity and sulfate in the seep cores obtained from Sites 7 and 8 (Figs. 11 and 12). Microelectrode profiles also indicated that dissolved oxygen (Fig. 8) was present in the upper 1 cm of the sediment and sulfide concentrations (Fig. 10) in the upper 10 cm were rather low, compared to those of seeps in other regions (e.g., Rathburn et al., 2003).

4.3.4.3. Carbonate rock geochemistry. Samples of carbonate rocks were collected in the area of methane seepage, characterized by the presence of clams and pogonophorans (Sites 7 and 8). Most of these rocks were exposed on ledges on the canyon walls. We recovered four rock specimens and analyzed their carbonate chemistry and isotopic composition. These rocks represent a sediment assemblage that was cemented by carbonate. Most of these rocks consisted of high magnesium calcite (6–14 mol % $MgCO_3$; Table 4). Using the approach outlined by Gieskes et al. (2005), we have corrected the measured $\delta^{18}O$ value for Mg-content (courtesy Dr. Jens Greinert, University of Bremen). The $\delta^{18}O$ (PDB) were corrected for $MgCO_3$ after Friedman and O'Neil (1977; see also Gieskes et al., 2005).

4.3.5. Megafauna

Representatives of eight phyla were observed in the seabed photographs. These included poriferans, cnidarians, echiuroids (only along the slope sites), arthropods, molluscs, echinoderms,

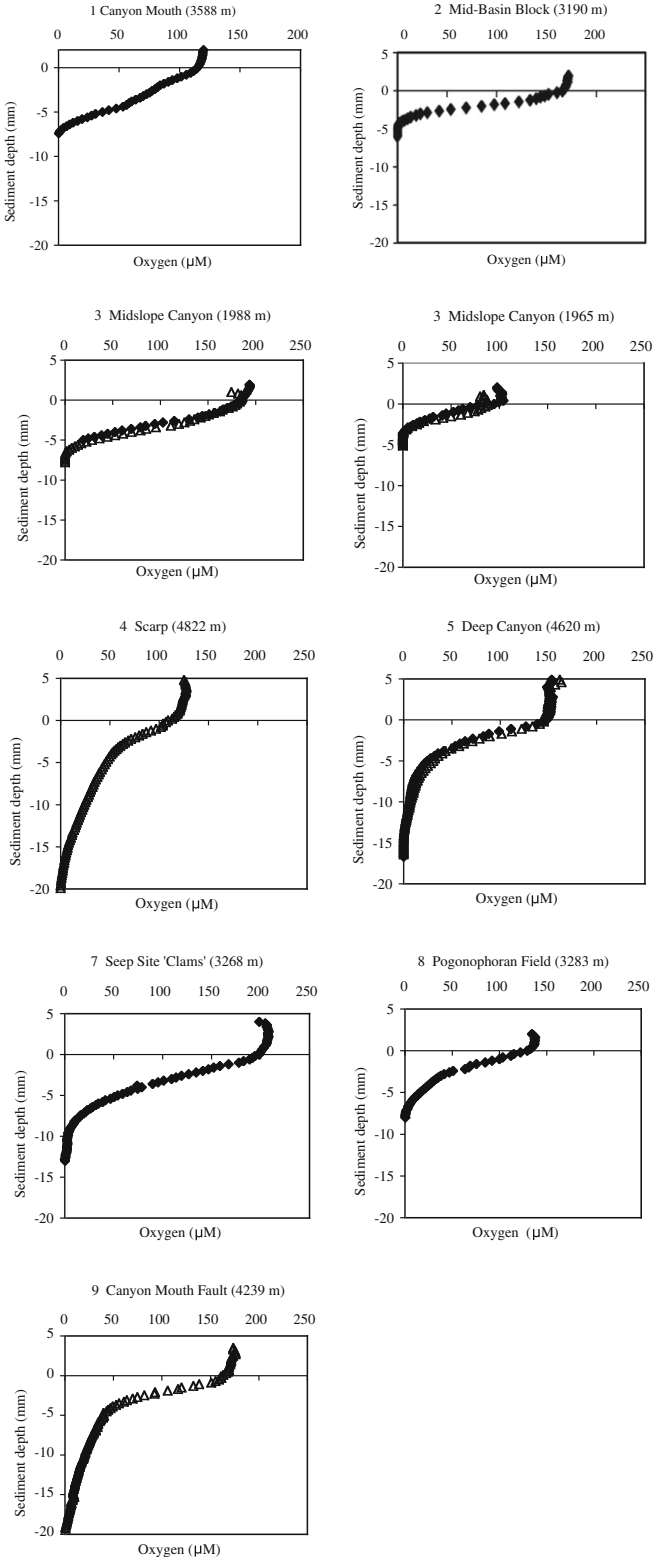

Fig. 8. Oxygen microprofiles measured in intact cores at 250 μm vertical intervals.

hemichordates (only on the abyssal plain) and chordates (Table 2). Total megafaunal densities were significantly different among transects ranging from 0.265 to 5.38 (individuals m^{-2}) from deepest to shallowest ($P < 0.0001$). The echinoderms were the dominant phylum along each transect, making up 71.6%, 73.8%, 90.3% and 55.9% of the megafauna over the mid-basin block, the

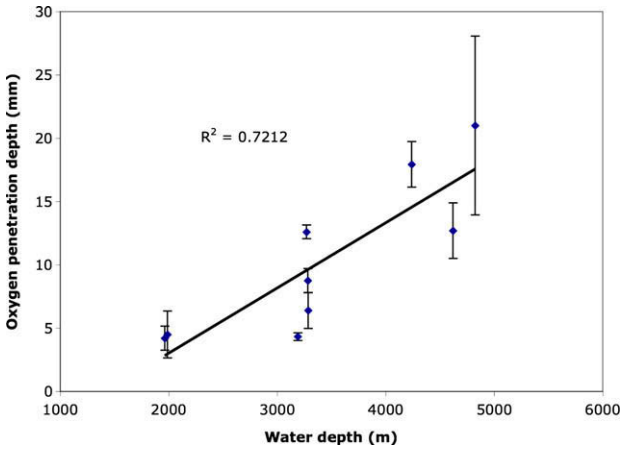

Fig. 9. The relationship between water depth and penetration depth of oxygen into the sediments. Values are shown as average penetration depths of 3–5 profiles measured at the same sites. Variations are illustrated as the standard deviations.

slope at 3200 m, the slope at 2000 m and the terrace basin, respectively. Within the echinoderms, dense beds of ophiuroids (88.6% of total megafauna) dominated at 2000 m, while echinoids (39.4–39.9%) and ophiuroids (20.8–23.3%) shared dominance at the 3200 m sites. Over the terrace basin at 4200 m, soft-bodied megafauna representing the holothuroids (47.2%) and actinians (11.3%) were most abundant. Based upon these patterns, the mid-basin block summit and slope transect at 3200 m were represented by similar megafaunal communities (Fig. 14), while the shallower slope and abyssal terrace basin sites appeared more distinct.

Because three distinct bottom types were observed along the 3200-m slope transect, we also examined the distinctness of the megafaunal communities among soft-sediment, sediment-rock outcrop mix and rock outcrop bottoms. While all habitats we observed at 3200 m were still dominated by the echinoderms, rock outcrop communities had more ophiuroids and crinoids and appeared distinct from both soft-sediment and sediment-rock outcrop mix bottoms (Fig. 15). Echinoids were most consistently observed over non-outcrap bottoms, along with elasipods (soft-sediment) and the Porifera (sediment-outcrop mix).

4.3.6. Macrofauna

Aleutian margin macrofauna were relatively abundant for the water depths considered (1965–4822 m), with densities ranging from roughly 2000 to 11,000 ind m^{-2} (0.3 mm mesh) (Table 5). Significantly higher densities were observed at the pogonophoran field and the shallowest canyon site (1965 m), than at Sites 2 (Mid-basin block), 5 (4620 m canyon) and 7 (clam beds), but no other site differences were found ($F_{7,22} = 6.79$; $P = 0.001$).

Each site sampled had a different suite of dominant taxa (Table 5), reflecting highly heterogeneous community composition on the margin. The Midslope Canyon macrofauna (Site 3, 1965 m) was dominated by cumaceans (27%) with acrocirrid, paraonid and cossurid polychaetes and nemerteans each contributing about 9% of the total. The midslope (Site 6, 3300 m) and the isolated Mid-basin block (Site 2, 3200 m) differed in faunal composition despite similar water depths. Ampharetid and cirratulid polychaetes each formed 13% of the fauna on the slope, with tanaids and cossurids also abundant. In contrast, paraonid polychaetes (29%) and gammarid amphipods (17%) formed most of the mid-basin block fauna. The seep sites, at similar depths (3267–3283 m), exhibited different infaunal communities in the clam bed and pogonophoran field habitats. Tanaids were 20% and paranoid and ampharetid polychaetes each formed 11% of the clam bed infauna. Gastropods (36%) and nemerteans (10%) were dominant in the pogonophoran fields. The deeper canyon and scarp sites (3580–4822 m) were characterized by large numbers of tanaids (10–38%) as well as abundant spionid and cirratulid polychaetes (Table 5).

Isotopic signatures for macrofauna at non-seep sites at 1965–4822 m (in shallow canyons and on the mid-basin block summit) reflected a phytoplankon-based diet ($\delta^{13}C = -16.7$–18.1; $\delta^{15}N = 11.7$–15.7) (Fig. 16). Average macrofaunal isotope signatures were slightly lighter on the slope in the vicinity of the seeps ($\delta^{13}C = -19.8$; $\delta^{15}N = 10.9$) and in a deep canyon ($\delta^{13}C = -20.3$; $\delta^{15}N = 9.76$), but not significantly so. Macrofaunal signatures were considerably lighter in pogonophoran field sediments (on average $\delta^{13}C = -26.22 \pm 8.22$, $\delta^{15}N = 6.85 \pm 6.01$), and in the vesicomyid clam beds ($\delta^{13}C = -33.65 \pm 12.20$; $\delta^{15}N = 8.66 \pm 4.06$) relative to the other habitats (Kruskal–Wallis/Tukeys HSD test; df = 7; $P < 0.0001$ for both $\delta^{13}C$ and $\delta^{15}N$), indicating chemosynthesis-based nutrition based largely on sulfide oxidation (Fig. 16). Among individual taxa, the nematodes of the family Leptosomatidae (identification by W. Decraemer, Royal Belgian Institute of Natural Sciences, Vautierstraat 29, B-1000 Brussels, Belgium; September, 2005) ($\delta^{13}C = -42$ to -43), Nereidae ($\delta^{13}C = -57$), Phyllodocidae ($\delta^{13}C = -52$) and capitellid polychaetes ($\delta^{13}C = -60$ to -66) had signatures suggestive of reliance on methane-derived carbon.

4.3.7. Reef epifauna

Most of the rocks visible on the Unimak margin appeared to be lithified sediment and supported only sparse numbers of filter feeding epifauna (Fig. 2d). However, several carbonate boulders adjacent to the clam bed sites were covered with dense aggregations of sessile epifauna. These appeared to include cnidarians, polychaetes, hydroids, corals and sponges, as well as mobile predators such as octopus. Most of the sessile forms were oriented downward, as if feeding on materials emanating from the seep (Fig. 2b). Limited sampling suggests that epifauna living on the rocks immediately adjacent to the seep (hydroid, bamboo coral, *Bathypathes* sp.) had lighter $\delta^{13}C$ signatures (-24.24 ± 0.9, $n = 3$) but similar $\delta^{15}N$ signatures (10.6 ± 0.9, $n = 3$) as animals collected on rocks further away on the same dive ($\delta^{13}C = -17.8 \pm 1.4$; $\delta^{15}N = 11.4 \pm 0.9$, $n = 4$) or on the adjacent slope off the seep ($\delta^{13}C = -18.4 \pm 0.8$; $\delta^{15}N = 10.2 \pm 1.3$, $n = 6$). We noted that *Bathypathes* sp. collected on the summit block at 3190 m had a heavier $\delta^{13}C$ signature ($-20.7‰$) than the same species collected on the rock overhanging the seep ($-22.8‰$) at 3260 m.

4.3.8. Foraminifera

Vertical distribution patterns of living (rose Bengal-stained) benthic foraminifera (>150 μm) analyzed within tube core sediments showed patterns comparable to other regions, though influenced by disturbances such as turbidity currents and methane seeps. At a bathyal site (1988 m water depth) the agglutinated assemblage had a density maximum at the 0–1 cm interval, while calcareous standing stocks of foraminifera had an infaunal maximum (Fig. 17). Infaunal patterns observed at this site were similar to those observed in similar water depths elsewhere (e.g., Rathburn and Corliss, 1994). Dominant infaunal taxa included: *Globobulimina pacifica*, *Nonionella stella*, *Nonionella globosa*, *Elphidium sp.* and *Chilostomella oolina* (Fig. 18). At this site, the deep infaunal species *G. pacifica*, reached unusually high densities (about 90 individuals 50 cm^{-3}) between 3 and 5 cm deep.

Comparisons revealed similar vertical distribution patterns (Fig. 17) of foraminifera (>150 μm) between cores taken from a cold methane seep (3283 m water depth; Site 8) and a nearby, non-seep site (3310 m; Site 6). Agglutinated foraminifera constituted more than 90% of the total foraminiferal assemblage at both sites (Fig. 18). Of the agglutinate assemblages at the non-seep site (Site 6), *Reophax* had a surface (0–1 cm) density maximum and a density maximum within the top 2 cm at the seep site (Site 8).

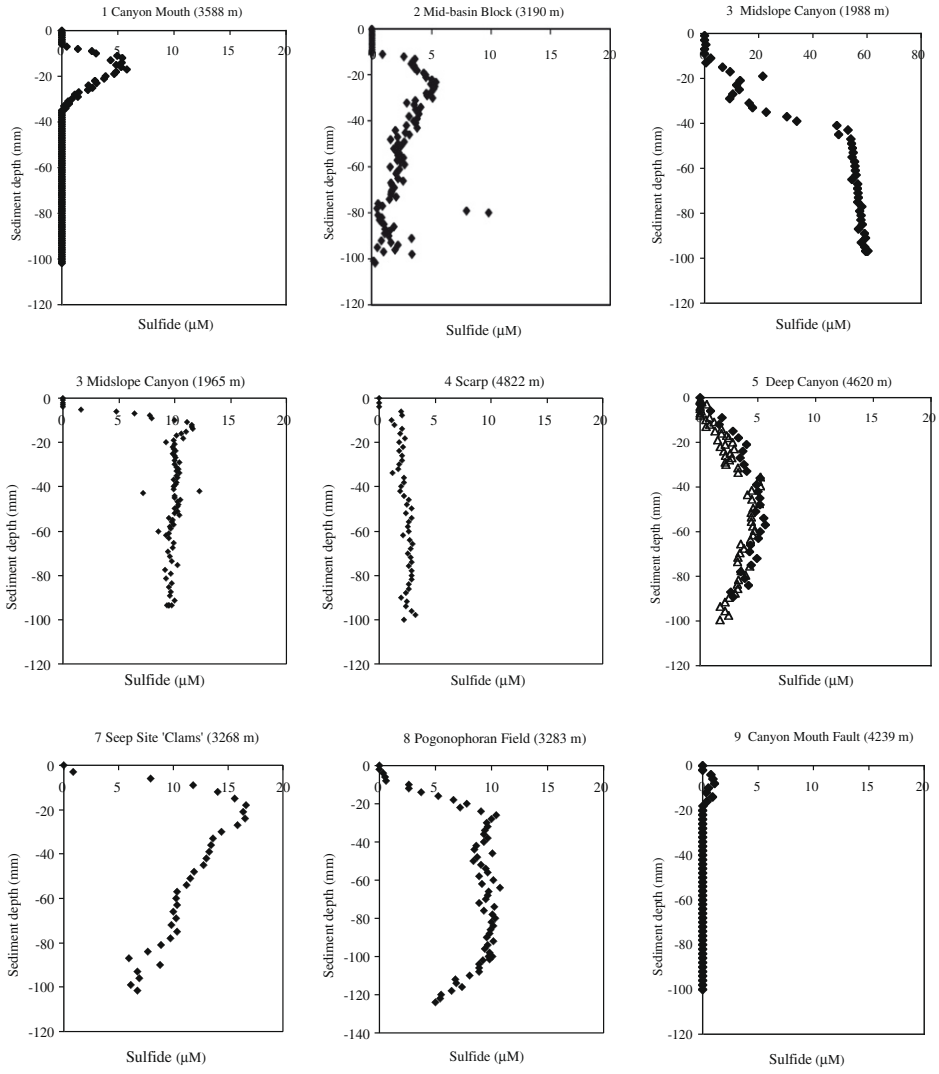

Fig. 10. Hydrogen sulfide microprofiles measured in intact cores at 1 mm vertical intervals.

Rhabdammina, *Recurvoides* and *Trochammina* had maximum densities at 1.5 cm or deeper within the sediment. Within the calcareous assemblages, numerous specimens of *Cibicides wuellerstorfi* were found attached to pogonophoran tubes associated with the seeps (Site 8). Of special interest is the occurrence of the typically shallow water calcareous taxon, *Elphidium*, in the topmost cm at both sites.

5. Discussion

Analyses of the geological features evident from the multibeam sonar data (Fig. 1h) show a heterogeneous seafloor characterized by canyons, faulting and sediment transport, however, we found no single slide in the study area that is comparable to the projected size of the Ugamak Slide. There was, however, extensive evidence for other and smaller-scale forms of disturbance such as current scouring and bioturbation. Methane seeps were also found at one site in water depths of 3267–3284 m. Sediment X-radiographs and digital images show layering, shell fragments and apparent mud clasts in the upper 10 cm of some cores (Figs. 3 and 4). These are all suggestive of relatively recent sediment disturbance, probably by redeposition, though bioturbation may also have played a role.

5.1. Major habitats

5.1.1. Canyons

Sediments from canyon environments in the study area were characterized by relatively higher organic matter availability (as indicated by TOC, TN, C:N ratio, CPE and chl *a*:TOC ratio) compared to slope or basin environments and the presence of bivalve shell material, burrows, and mottling. High organic contents also correlate with highest counts of microorganisms in surface sediments. Deep canyon sediments had abundant shell fragments, suggesting transport and redeposition. Any X-radiograph evidence of transport would have been obscured by bioturbation in sediments from the canyon sites at 1988 m (Site 3) and 3588 m (Site 1). Canyon communities were dominated by ophiuroids and crinoids, and as a result, were highly distinct from both soft-sediment and sediment-rock outcrop mix bottoms (Fig. 14). In the Midslope Canyon (Site 3), foraminiferal assemblages were dominated by calcareous taxa, with relatively high abundances of infaunal taxa, including the deep infaunal species, *Globobulimina pacifica*. Microprofiles indicate that only porewaters in the upper 2 cm were oxic. The occurrence of deep infaunal taxa (Figs. 17 and 18) below the porewater oxic zone is common (e.g., Rathburn et al., 1996; Fontanier et al., 2005), and may reflect food preferences and their potential

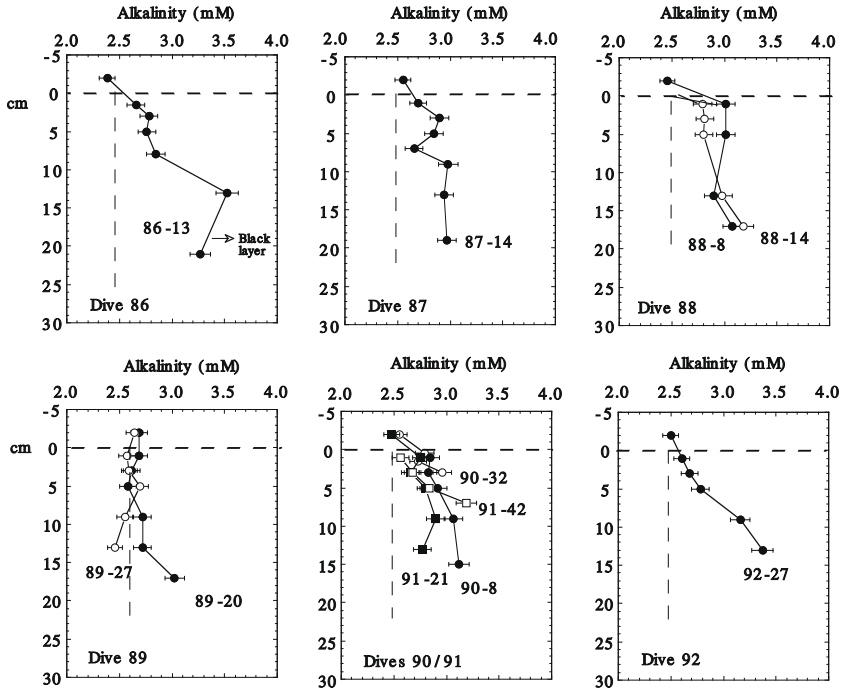

Fig. 11. Alkalinity profiles in cores. Numbers adjacent to the profiles represent dive number and core number from which the porewater was extracted. Two cores were collected in similar environments at Site 3 in dives 88 and 89 (88-8 (1964 m) and 88-14 (1988 m). For dive 89, core 89-20 (4822 m) was collected at Site 4 and core 89-27 (4620 m) was collected at Site 5. During dive 90, core 90-8 (3310 m) was collected at Site 6, and core 90-32 (3268 m) was collected at the edge of a clam bed (Site 7). Core 91-42 (3280 m) was collected in a separate clam bed (Site 8.5), while core 91-21 (3284 m) was collected in the pogonophoran field (Site 8).

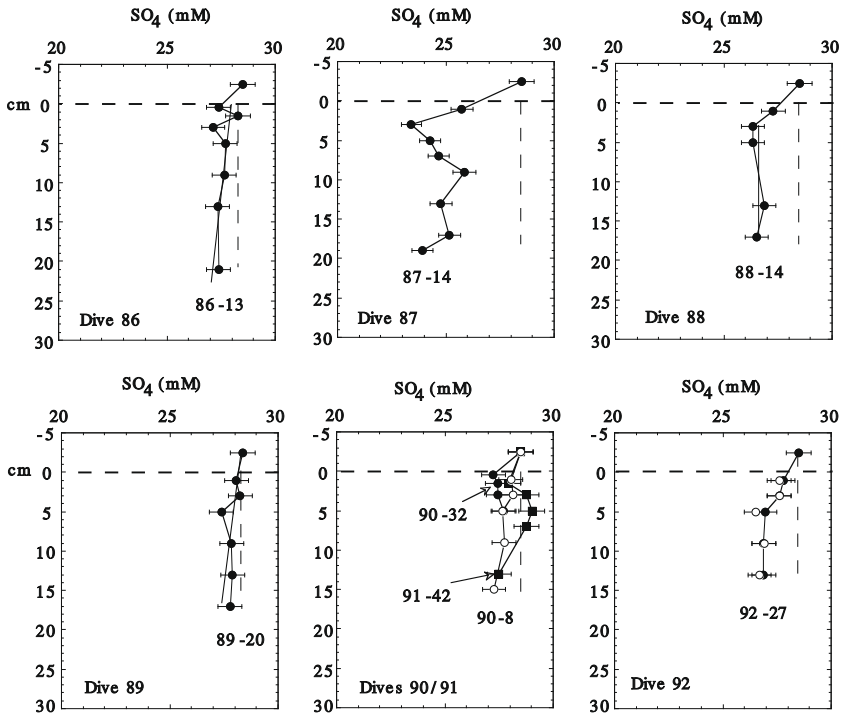

Fig. 12. Sulfate profiles in cores. Vertical broken lines represent bottom water values. Numbers adjacent to the profiles represent dive number and core number from which the porewater was extracted. Two cores were collected in similar environments at Site 3 in dives 88 and 89 (88-8 (1964 m) and 88-14 (1988 m). For dive 89, core 89-20 (4822 m) was collected at Site 4, and core 89-27 (4620 m) was collected at Site 5. During dive 90, core 90-8 (3310 m) was collected at Site 6, and core 90-32 (3268 m) was collected at the edge of a clam bed (Site 7). Core 91-42 (3280 m) was collected in a separate clam bed (Site 8.5), while core 91-21 (3284 m) was collected in the pogonophoran field (Site 8).

capacity to use nitrate to respire (as indicated for *Globobulimina pseudospinescens*; see Risgaard-Petersen et al., 2006).

Relatively high abundances of infaunal foraminifera in the shallow canyon imply ample supplies of buried organic material

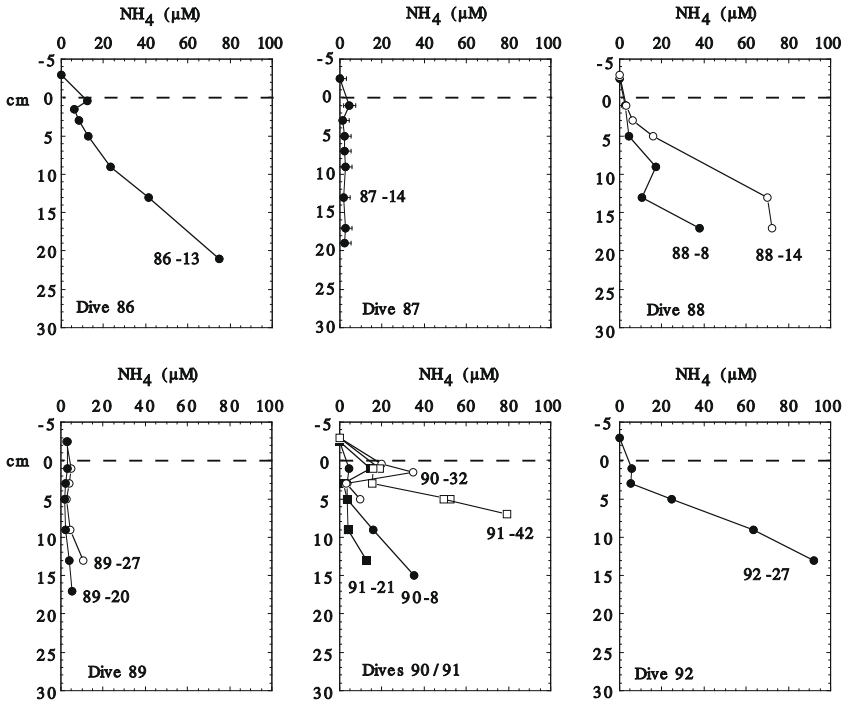

Fig. 13. Ammonium profiles in cores. Numbers adjacent to the profiles represent dive number and core number from which the porewater was extracted. Two cores were collected in similar environments at Site 3 in dives 88 and 89 (88-8 (1964 m) and 88-14 (1988 m). For dive 89, core 89-20 (4822 m) was collected at Site 4, and core 89-27 (4620 m) was collected at Site 5. During dive 90, core 90-8 (3310 m) was collected at Site 6, and core 90-32 (3268 m) was collected at the edge of a clam bed (Site 7). Core 91-42 (3280 m) was collected in a separate clam bed (Site 8.5), while core 91-21 (3283 m) was collected in the pogonophoran field (Site 8).

Table 4
Carbon and oxygen stable isotope values and $MgCO_3$ mole percentages of carbonate rocks collected in the study area. Oxygen isotope values corrected for $MgCO_3$ are also included in the right-hand column. $\delta^{18}O$ (PDB) corrected for $MgCO_3$ after Friedman and O'Neil (1977).

Sample	Carbonate isotope data			
	$\delta^{13}C$ (PDB)	$\delta^{18}O$ (PDB)	$MgCO_3$ (mol %)	$\delta^{18}O$ (PDB) corrected
90-1	−17.25	5.10	11	4.40
90-1-1	−29.84	5.53	13	4.75
90-1-2	−32.34	5.41	14	4.57
90-1-3	−33.59	5.60	13	4.82
90-2	−16.68	5.02	11	4.36
90-2-1	−33.14	4.86	6	4.50
91-2	−26.03	3.93	6	3.57

as direct or indirect sources of food. The presence of labile organic material within the sediments at this Site (3) is supported by the relatively high infaunal microbial abundances (Fig. 6; 1988 m) and the presence of relatively high surface sediment CPE values (Table 3; 1965 m). Foraminiferal assemblages found in the deeper canyon sites were dominated by agglutinated taxa, as is often the case in waters below 3000 m in the Pacific (e.g., Gooday, 1999). Macrofaunal assemblages differed in each canyon, with cumaceans dominant in the shallowest canyon (Site 3) and tanaids and/or polychaetes dominant in the deeper scarps and canyons (Sites 4, 5 and 9; Table 5). Cumaceans can be characteristic of sites with significant sediment motion and are known to rapidly colonize disturbed or enriched sediments at bathyal depths (Snelgrove et al., 1994; Levin et al., 2006).

5.1.2. Mid-basin block summit – a topographic high

The summit of the isolated, Mid-basin block (Site 2) was characterized by compacted sediments. Density variations in the X-radiograph indicate that mud rip-up clasts were present (Fig. 3c). The summit of this feature was also distinct from other transects in having comparatively low Lebensspuren densities (Table 2). A number of explanations for this are possible, including the idea that the mid-basin block summit is disturbed by strong turbidity currents that either limit the abundance of benthic fauna, or rework sediment to remove Lebensspuren. Predation pressure may also be a factor as the mid-basin block transect was observed to have the second highest densities of fish (second to the 2000 m slope site), and the highest proportional abundance of fish (Chordates; Table 2).

Densities of the echiuroids, echinoderms and urochordates appeared more similar to the abyssal transect, suggesting that there is some influence of "deeper" fauna on the summit of the mid-basin block community (Fig. 14 and Table 2). In other words, echiuroids, echinoderms and urochordates were present in appreciable densities in both abyssal and mid-basin block environments, and there may have been interactions between some populations from these habitats. Proximity and small-scale dispersal may explain the similarities between the mid-basin block and abyssal environments. The mid-basin block summit is isolated from the slope by ~30 km but is <5 km from the 4200 m isobath. Thus, organisms with wide bathyal tolerances may move up from deeper depths on to the mid-basin block looking for food.

The summit of the Mid-basin block (Site 2) exhibited high dominance within the macrofaunal community, with paraonid polychaetes and gammarid amphipods together comprising 46% of the fauna (Table 5). As the most oligotrophic site studied, with the lowest sediment microbial counts and organic matter contents, this dominance was unexpected, and we speculate that this reflects a high degree of physical disturbance.

5.1.3. Seep ecosystem

Physically, seep sites discovered off Unimak Island were more varied than those previously encountered off Kodiak Island in the

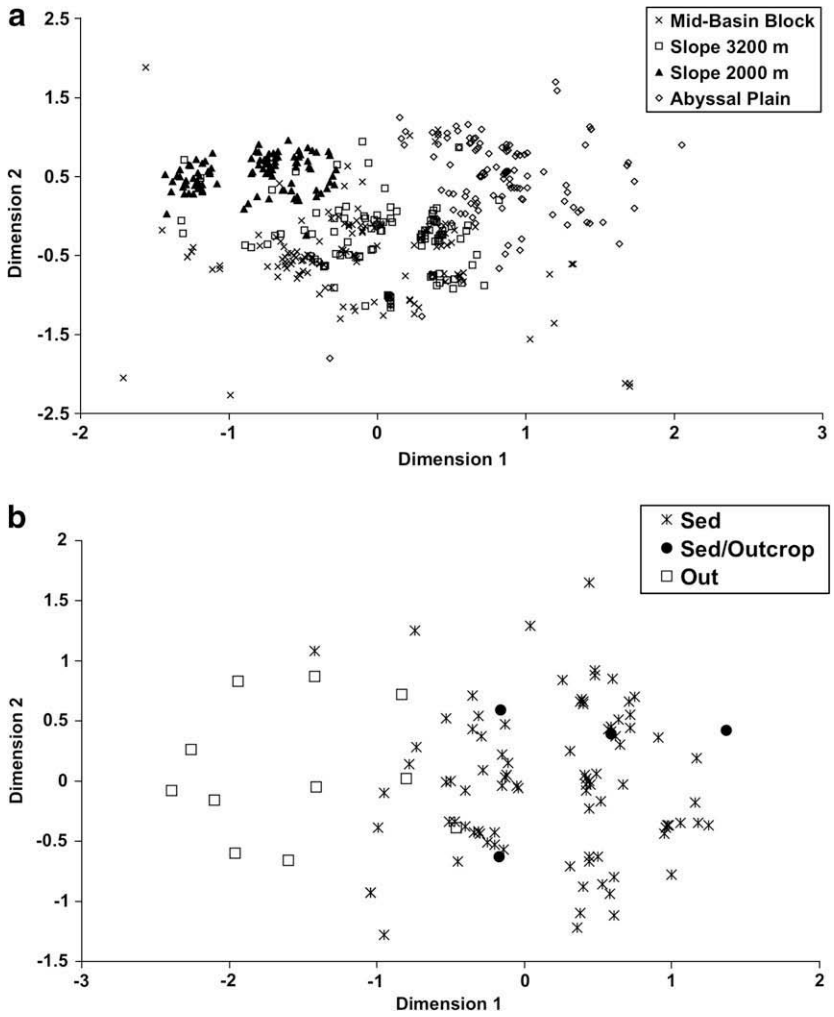

Fig. 14. Megafauna. (a) MDS plot of megafaunal assemblages over a basement block summit at 3200 m (Tow 1), the continental slope at 3200 m (Tow 2), the continental slope at 2000 m (Tow 3) and a terrace basin at 4200 m (Tow 4). MDS stress = 0.17; (b) MDS plot of megafauna assemblages over soft-sediment (Sed), sediment-outcrop mix (Sed/Out), and outcrap (Out) bottoms. MDS stress = 0.21.

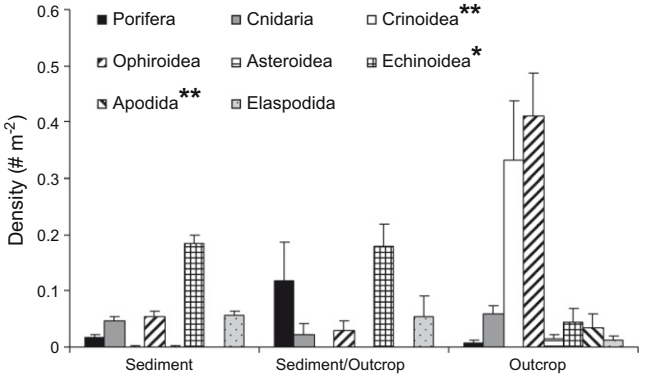

Fig. 15. Densities of megafauna at the 3200 m slope site (±1 SE) among sediment, sediment-rock outcrop mix and rock outcrop bottom types. Statistical differences among habitats for individual taxa based on Kruskal–Wallis test are denoted by $^{*}p < 0.05$ and $^{**}p < 0.01$.

Gulf of Alaska (4445 m; Levin and Mendoza, 2007). Both the Aleutian margin seeps and deep-water seeps occurring off Kodiak Island consisted of relatively small, isolated clam beds and patches of pogonophoran tubes that occurred in shallow sediments overlying rocky outcrops near a scarp. In both areas seepage may have occurred over a wider geographic range – either a function of previous seep habitats or more diffuse seepage that did not support clam beds or pogonophoran fields at the sediment–water interface. However, rocky outcrops overhanging the Aleutian margin seep sediments supported abundant life ("weeping rocks") (Fig. 2b) compared to outcrops located away from seepage (Fig. 2d) or off Kodiak Island.

The $\delta^{18}O$ values of the sampled carbonate rocks (Table 4) were indicative of temperatures that are much higher than present day bottom-water temperatures, consistent with the idea that these rocks formed deeper in the sediment column (cf., Gieskes et al., 2005) in waters of $\delta^{13}C$ (DIC) between −18 and −40‰ (PDB). At a later stage venting may have occurred, preferably in zones of rock exposure, as a result of uplift and/or slumping on canyon walls, similar to the processes proposed for some Monterey Bay seeps (Martin et al., 2004; Paull et al., 2005a,b). The location of authigenic rocks plays a critical role for deep-sea communities requiring hard substrate. We speculate that the composition, location and formation of authigenic carbonate rocks may also play an appreciable, but as yet unstudied, role in the distribution, biogeochemistry and composition of some deep-sea communities.

Based on porewater geochemical constituents (Figs. 11–13), we suggest that in the areas of methane seepage (Sites 7 and 8), either

Table 5
Macrofaunal densities (1 ± SE) and dominant taxa.

Station	1	2	3	4	5	6	7	8	9
Habitat	Canyon mouth	Mid-basin block	Midslope Canyon	Scarp	Deep canyon	Flat slope	Seep (cam bed)	Pogonophoran field	Canyon Mouth Fault
Depth (m)	3600	3190	1965	4822	4620	3310	3267	3283	3580–4240
No. of Cores	0	3	3	1	4	3	3	3	4
Mean No. ind m^{-2} (SE)	No data	3205 (1525)	11,156 (1675)	3883	2095 (727)	5362 (185)	2835 (888)	9738 (2342)	4114 (323)
Rank 1 Taxon		Paraonidae	Cumacean	Tanaid	Cirratulid/ Tanaid	Tanaid	Tanaid	Gastropoda	Spionidae
Taxon percentage									
Annelida									
Tubificidae		0.038	0.011	0.000	0.088	0.023	0.043	0.006	0.045
Siboglinidae		0.000	0.000	0.000	0.000	0.000	0.000	0.006	0.000
Polynoidae		0.019	0.011	0.000	0.000	0.011	0.043	0.006	0.034
Ampharetidae		0.096	0.011	0.000	0.059	0.126	0.109	0.025	0.000
Sphaerodoridae		0.000	0.000	0.000	0.029	0.000	0.022	0.006	0.011
Acrocirridae		0.058	0.094	0.000	0.000	0.011	0.043	0.013	0.011
Ophyrotrocha platykephale		0.000	0.000	0.000	0.000	0.000	0.000	0.006	0.000
Other Dorvilleidae		0.000	0.017	0.000	0.000	0.011	0.000	0.000	0.022
Paraonidae		0.288	0.083	0.000	0.029	0.046	0.109	0.013	0.079
Lumbrineridae		0.000	0.011	0.000	0.029	0.034	0.043	0.000	0.011
Cossuridae		0.000	0.088	0.000	0.029	0.092	0.043	0.013	0.112
Maldanidae		0.000	0.000	0.000	0.029	0.034	0.043	0.006	0.011
Ophelliidae		0.000	0.000	0.095	0.059	0.034	0.000	0.019	0.011
Prionospio spp.		0.000	0.000	0.238	0.000	0.011	0.022	0.000	0.022
Other Spionidae		0.019	0.017	0.000	0.088	0.057	0.000	0.019	0.180
Hesionidae		0.000	0.055	0.000	0.000	0.000	0.022	0.013	0.011
Cirratulidae		0.058	0.011	0.000	0.176	0.138	0.065	0.032	0.112
Capitellidae		0.019	0.000	0.000	0.000	0.011	0.000	0.013	0.000
Sabellidae		0.000	0.000	0.000	0.059	0.000	0.000	0.006	0.000
Syllidae		0.019	0.000	0.000	0.000	0.011	0.000	0.013	0.022
Phyllodocidae		0.038	0.000	0.000	0.000	0.011	0.000	0.000	0.011
Sigalionidae		0.000	0.006	0.000	0.000	0.000	0.000	0.000	0.011
Sternaspidae		0.000	0.011	0.000	0.000	0.000	0.000	0.000	0.000
Fauveliopsidae		0.000	0.000	0.048	0.000	0.000	0.000	0.000	0.000
Unid. Polychaete		0.000	0.017	0.095	0.059	0.034	0.043	0.013	0.011
Crustacea									
Cumacea		0.038	0.271	0.000	0.000	0.023	0.000	0.019	0.011
Isopoda		0.000	0.066	0.048	0.000	0.057	0.022	0.025	0.011
Tanaidacea		0.038	0.006	0.380	0.147	0.115	0.196	0.095	0.101
Gammarid Amphipod		0.173	0.028	0.000	0.029	0.011	0.022	0.032	0.011
Mollusca									
Acharax sp.		0.000	0.000	0.000	0.000	0.000	0.000	0.006	0.000
Other Bivalvia		0.038	0.055	0.000	0.029	0.011	0.065	0.025	0.045
Gastropod sp. A		0.000	0.000	0.000	0.000	0.000	0.000	0.177	0.000
Gastropod sp. B		0.000	0.000	0.000	0.000	0.000	0.000	0.025	0.000
Gastropod spp.		0.000	0.000	0.000	0.000	0.000	0.000	0.158	0.000
Aplacophora		0.000	0.006	0.000	0.059	0.011	0.022	0.019	0.022
Scaphopod		0.000	0.011	0.048	0.000	0.023	0.000	0.051	0.011
Other Taxa									
Ophiuroidea		0.019	0.017	0.048	0.000	0.000	0.000	0.006	0.022
Nemertea		0.019	0.088	0.000	0.000	0.034	0.000	0.101	0.011
Anthozoa		0.000	0.011	0.000	0.000	0.000	0.000	0.006	0.000
Hydrozoa		0.000	0.000	0.000	0.000	0.000	0.000	0.019	0.000
Sipunculida		0.019	0.000	0.000	0.000	0.011	0.022	0.000	0.000
Unidentified		0.000	0.000	0.000	0.000	0.000	0.000	0.006	0.000
Total No. of Individuals		52	181	21	34	87	46	158	89

aerobic methane oxidation dominates anaerobic oxidation (AOM) in the surface sediment, or anaerobic processes occur at deeper levels. This may result in part, from bioturbation in the upper sediments (note that penetration of the cores was often less than 20 cm). This was typically observed at the methane seep sites visited in our previous dives at ~4500 m in the Kodiak area (see Gieskes et al., 2005; Levin and Mendoza, 2007).

Levin and Mendoza (2007) compared Unimak seep macrofauna to those at deep seeps off Kodiak Seamount in the Gulf of Alaska (4445 m) and the Florida Escarpment in the Gulf of Mexico (3300 m). The Unimak fauna differed from the other seep settings in being crustacean- rather than annelid-dominated. We hypothesize this reflects the relatively low levels of sulfide and possibly limited methane flux rates in Unimak sediments, as well as sediment disturbance. The Unimak seep fauna had lower rank 1 dominance and greater species richness and diversity (H') per core (Levin and Mendoza, 2007). However, seep macrofaunal densities were not elevated above background (non-seep) levels at either the Unimak or Kodiak seep sites.

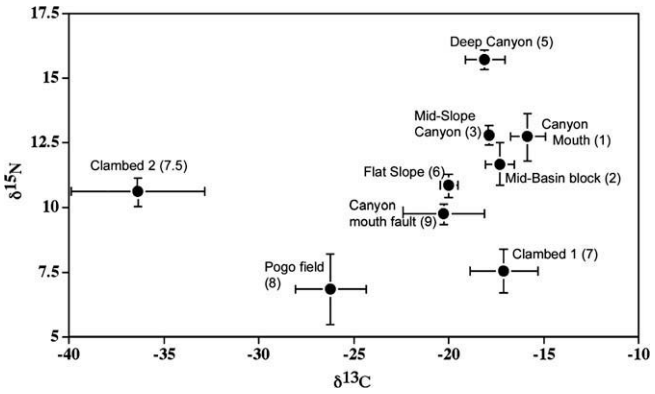

Fig. 16. Carbon and nitrogen stable isotopic compositions of macrofauna from Unimak margin habitats.

Nutritional patterns in Unimak macrofauna reflect small-scale heterogeneity in food sources, with clam bed and pogonophoran field seep patches having distinctive chemosynthetic inputs (Fig. 16). A comparison of infaunal communities from deep (>3000 m) seeps at Kodiak (4450 m), Unimak (3260–3280 m) and the Florida Escarpment (3200 m) revealed that the Unimak system exhibited the least dependence on chemosynthesis of the three regions. Levin and Mendoza (2007) estimated methane contribution to macrofaunal carbon pools to be low in the Unimak pogonophoran field (9%) and higher (22%) in the Unimak clam bed, but notably less than observed at deep seeps off Kodiak Island and Florida Escarpment (26–44% depending on the habitat). Megafaunal abundances were relatively high along the Aleutian margin, as compared with sites of similar depth and proximity to land in the Atlantic Ocean as summarized by Levin and Gooday (2003). Although no seeps were observed in the photo-transects, we can speculate whether seep production is being incorporated by vagrant predators or scavengers and then moved off site, leading to high overall densities along the margin (e.g., MacAvoy et al., 2002).

Observations from this study imply that at least some organisms residing on hard substrates in the deep-sea can obtain nutrition from chemosynthetic sources. This nutritional influence on populations living on rocks adjacent to methane seepage may appreciably influence the distribution of modern communities and those in the geologic record. The presence of dense communities on hard substrates near seeps on the Aleutian margin and isotope data indicating that deep-sea reef cnidarians (e.g., corals and hydroids) residing on rocks near seepage may obtain some nutrition from chemosynthetic sources suggest that methane seeps can affect organisms living above the sediment–water interface. High cover and high density of epibenthic megafauna on rocks, while expected in the intertidal zone and in shallow reefs, are typically uncommon at depths of >3000 m, even on seamounts (Heezen and Hollister, 1971; Lundsten et al., in press). Observations near the Unimak seep site suggest a heretofore unexplored nutritional influence of methane seepage on background reef faunas, in addition to the provision of hard substrate.

In the Unimak (Fig. 18) and Kodiak (Rathburn, unpublished data) study areas, seep and non-seep foraminiferal assemblages were both dominated by agglutinated taxa. The presence of calcareous foraminifera in seeps on the Aleutian margin probably results from the availability of habitat elevated above the seafloor (*Cibicides wuellerstorfi*) and resilient, acclimated shallow water taxa brought in by turbidity currents (*Elphidium* sp.). Of the dominant calcareous taxa, *Elphidium* sp. and *C. wuellerstorfi* had maxima at the 0–1 cm interval. Fifty percent of the *C. wuellerstorfi* found at the seep site were attached to pogonophoran tubes that extended above the sediment–water interface. This taxon prefers an elevated habitat (e.g., Mackensen et al., 2006), and the presence of suitable

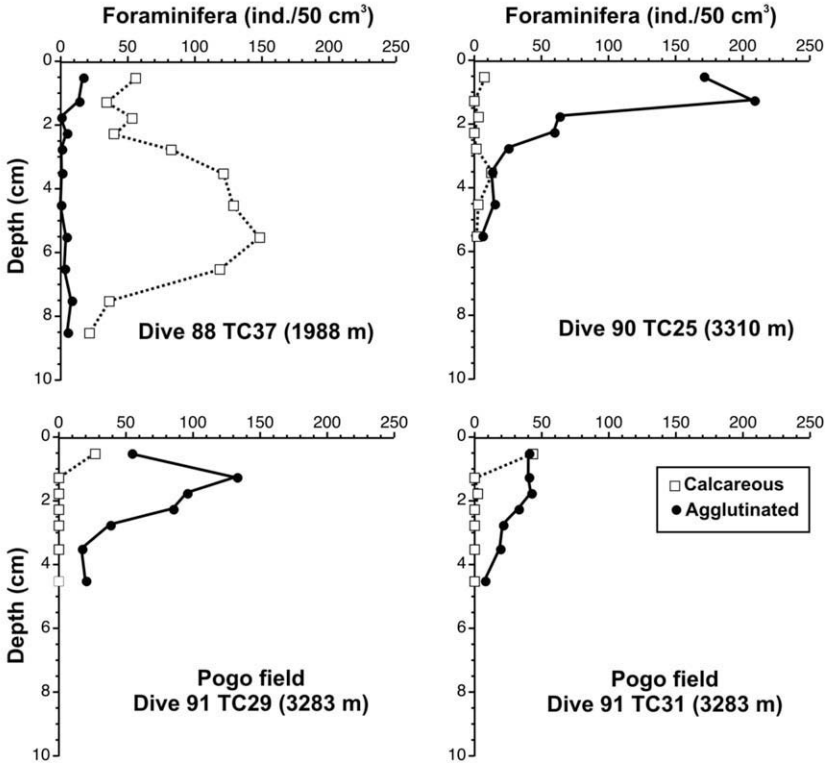

Fig. 17. Foraminiferal density profiles (number of individuals 50 cm^{-3}) of calcareous and agglutinated taxa within the sediments. Dive number, core number and water depth are provided; Core TC37 was collected from Site 3, TC25 was taken at Site 6, and TC29 and TC31 were taken from Site 8.

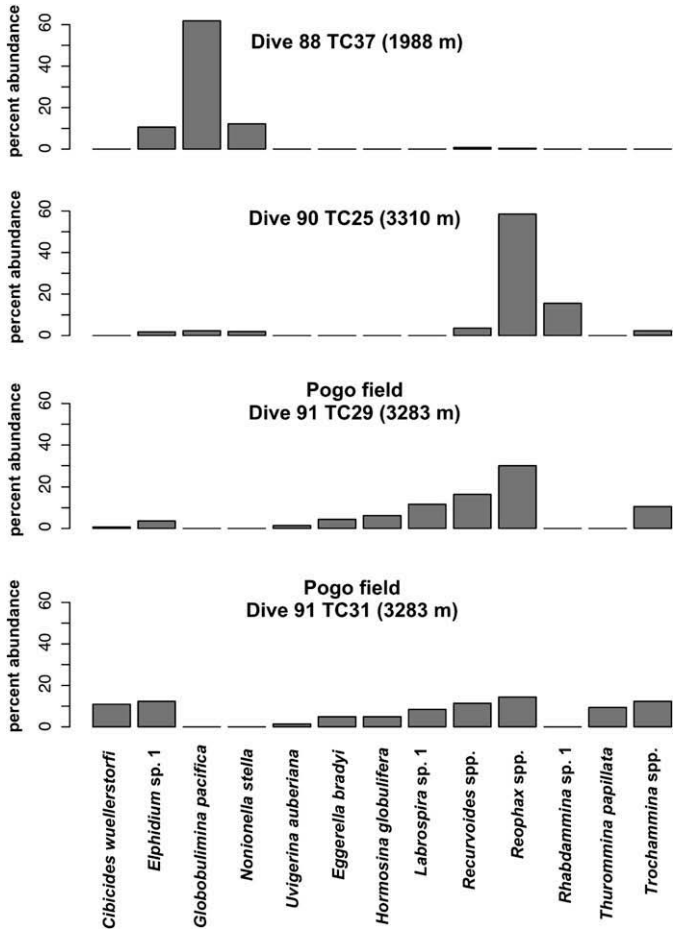

Fig. 18. Percent abundances of common foraminiferal taxa. Dive number, core number, and water depth are provided; Core TC37 was collected from Site 3 (1988m), TC25 was taken at Site 6, and TC29 and TC31 were taken from Site 8.

habitat on pogonophoran tubes extending above the sediment–water interface probably accounts for the abundance of *Cibicides* at this site.

5.2. Bathymetric trends

Global analyses suggest that megafauna and macrofauna dominate biomass on bathyal continental margins, but that their abundances exhibit exponential declines with water depth (Rex et al., 2006). Bacteria density and biomass in contrast, show no global declines with water depth (Rex et al., 2006). Foraminifera often constitute a large proportion of the biomass in deep-sea environments (e.g., Snider et al., 1984; Gooday et al., 1992), though below the Calcite Compensation Depth (CCD) calcareous taxa are not common and foraminiferal assemblages are dominated by agglutinated and soft-walled taxa (e.g., Gooday et al., 2008). Total macrofauna on the Aleutian margin exhibited a non-significant trend of decreasing densities with depth ($r^2 = 0.46$; $P = 0.06$). A similar negative relationship between water depth and density was evident for megafauna ($r^2 = 0.76$; $P = 0.13$), although this was not true for all individual taxa. Porifera for example, were most abundant along the deepest transect (Table 2). Also, there was a clear shift from ophiuroids to echinoids to holothurians as depth increased from 2000-3200-4200 m. Metabolically, maintaining calcium carbonate shells or ossicles becomes harder with increasing hydrostatic pressure (McClain et al., 2004; Gooday, 2002). This is a potential explanation for the shift from the heavily ossified ophiuroids and echinoids towards the soft-bodied holothurians with depth. Alternatively, the shifts in taxa may be indicative of changes in trophic or feeding mode strategies, with scavengers and suspension feeders on the upper and midslope being replaced by deposit and suspension feeders along the lower slope and continental rise (Gage and Tyler, 1999).

Habitat heterogeneity generated by canyons and methane seepage appear to influence food supply for microbes and macrofauna in ways that supersede any clear depth gradient in organic matter input or quality (depth vs %C, C:N, chl *a* or CPE, all $P >>> 0.05$). The shallowest station (Site 3; a canyon at 1965 m) and the pogonophoran field (3283 m) exhibited greatest macrofaunal densities, with communities comprised largely of cumaceans and gastropods, respectively. The Aleutian macrofaunal communities differ from many other continental margin assemblages by (a) having crustaceans rather than polychaetes as the dominant taxon and (b) exhibiting high dominance by single crustacean taxa. This may reflect overall elevated levels of sediment disturbance.

The community structure (density and composition) we observed between 2000 and 4600 m differed greatly from that reported by Jumars and Hessler (1976) for the deep Aleutian Trench. Although we employed a similar sieve size and sampled at similar latitude, they sampled deeper, in a flatter region further west, and used a USNEL box corer that could have blown many small crustaceans off the sediment surface. Macrofaunal densities on the Aleutian margin are at the upper end, but within the range of those observed at comparable depths in the Atlantic Ocean, where extensive margin sampling has been conducted (Levin and Gooday, 2003).

Bathymetric patterns of foraminifera within the study site correspond with those observed in other regions. Assemblages had appreciable numbers of calcareous taxa at depths around 2000 m (1965 and 1988 m), but changed to assemblages dominated by agglutinated taxa in deeper water depths. These changes probably result from a decrease in available food with depth and closer proximity to the lysocline (e.g., Gooday et al., 2008). In the Sulu and South China Seas, infaunal assemblages were dominated by calcareous taxa at 4000 and 4500 m sites influenced by turbidity currents (Rathburn et al., 1996). These taxa were apparently able to take advantage of labile, subsurface organic material transported from shallower depths by turbidity currents. Although we have not observed abundant calcareous infauna in the abyssal samples we have examined, there is some evidence that suggests the influence of transport from shallower environments (Fig. 18). The relatively high infaunal abundances of *G. pacifica* (Figs. 17 and 18) and microorganisms (Fig. 6), and high quality organic materials (Table 3) in the Midslope Canyon Site (1988 m) are suggestive of buried labile organic material, though bioturbation may also play a role in bringing organic material from the surface to infaunal habitats. Previous authors have suggested that *Globobulimina* species respond to the position of redox boundaries (see Jorissen, 1999). At least one *Globobulimina* species appears to use nitrate to respire, enabling this species to live in anoxic sediments for extended periods (Risgaard-Petersen et al., 2006). At least some *Globobulimina* species ingest clay and associated bacteria (Goldstein and Corliss, 1994), and there appears to be an abundance of infaunal microorganisms to feed upon at Site 3 (1988 m; Fig. 6). The presence of appreciable numbers of *Elphidium* sp. may also reflect transport from shallower habitats. *Elphidium* species are typically abundant in shallow environments, though they may also be found living in relatively low numbers in deep-sea environments (see Corliss, 1991). We suggest that the large percentage of *Elphidium* found in some samples reflects acclimation of specimens brought in by turbidity currents. Shallow-water materials traveling downslope in submarine canyons can deliver labile food and robust taxa to deep-water habitats. These deposits are known to have extended the depth ranges of some shallow water taxa, and may

provide suitable conditions for some taxa to flourish spectacularly (Vetter, 1995). *Elphidium* may be better able to acclimate to deep-water conditions and survive turbidity current (or slope or debris flow) transport than some other shallow water taxa. An ability to survive transport and acclimate to new conditions might explain why *Elphidium* is found living in deep-sea environments, especially those influenced by turbidity currents.

5.3. Organic matter influences

Much of the organic matter found on the deep-sea floor is ultimately derived from surface waters (e.g., Suess, 1980). The range of mean chlorophyll values of sea surface waters along the Aleutian margin during June–July (time of collection of cores) is about 3–5 mg m^{-3}. Estimates of primary productivity in the region ranged from 910 ± 150 and 770 ± 70 mg Cm^{-2} day^{-1} for June 2001 and 2002, respectively (Mordy et al., 2005). Oxygen penetration into the sediment increased slightly with increasing water depth (Figs. 8 and 9), suggesting reduced OM inputs and degradation, although C, N, C:N and pigment measures were uncorrelated with water depth (Table 3). As a likely result of the accumulation of organic carbon from sediment redeposition, oxic porewaters within the sediments did not penetrate as deep (up to 2 cm in the deeper station) as usually assumed for deep-sea environments (Fig. 9). Oxygen penetration into sediments has been reported to exceed 1 cm sediment depth in 1300 m water depth in other regions (Holby and Ries, 1996), and to reach several centimeters deep in water depths of >3000 m (Glud et al., 1994). In contrast, typical oxygen penetration depths in productive coastal environments do not exceed a few millimeters (Gundersen and Jørgensen, 1990). Carbon and nitrogen isotopic composition of sediments was also highly heterogeneous in different habitats (Fig. 5). It is unknown how much of the seasonal input of sea surface productivity reaches the sea floor along the Aleutian margin, but it is clear that redistribution of sea floor materials is typical in the region.

One effect of high relief or canyon topography is to focus currents and redistribute organic matter. The summit of the isolated Mid-basin block (Site 2) was clearly current swept and sediments exhibited reduction in organic matter quantity and quality relative to the slope at comparable depths (Site 6; Table 3). Macro- and megafaunal densities showed corresponding reductions relative to those at similar depths on the contiguous slope. Sites 3 and 9, both canyon locations but separated by over 2200 m water depth, exhibited the most pigment-rich sediments and among the highest non-seep microbial and macrofaunal densities. While no significant simple linear relationships were found between any measure of sediment organic matter availability or quality (% C, C:chl *a*, CPE) and abundance of macrofauna or megafauna, a combination of bacterial counts and chloroplastic pigments (CPE) accounted for 97% of variance in macrofaunal abundance (multiple regression: $r^2 = 0.97$; $P = 0.031$). As seen elsewhere (e.g., Gooday et al., 2008), agglutinated taxa generally dominate calcareous taxa in foraminiferal assemblages found in deeper-water habitats. Dominance of agglutinates probably results from a decrease in available food with depth (e.g., Gooday et al., 2008), which can be modified by local conditions such as hard substrates (e.g., Beaulieu, 2001), and seep habitats (e.g., Rathburn et al., 2003). Clearly a complex interplay of factors, in which food supply is modified by topographic features and associated flow environments, determine faunal abundances and composition on heterogeneous margins.

6. Conclusions

Our investigations revealed that the feature known as the "Ugamak Slide" is not a slide at all, and could not have caused the 1946 tsunami event. We found no single feature within the study area that was of a similar size. Rather, the Aleutian margin reflects a mosaic of environments, each with distinct biological communities. These environments appear subject to multiple sources of disturbance including methane seepage, bottom flows, sediment transport and redeposition. Faunal trends in abundance, composition and diversity reflect this disturbance.

Bathymetry clearly influenced some sediment properties. Oxygen penetration into the sediment increased slightly with increasing water depth, suggesting reduced OM inputs and degradation, although C, N, C:N and pigment measures were uncorrelated with water depth. However, as a likely result of the accumulation of organic carbon from sediment redeposition, oxic porewaters within the sediments did not penetrate as deep as usually assumed for deep-sea environments. Carbon and nitrogen isotopic composition of sediments was also highly heterogeneous in different habitats. Habitat heterogeneity generated by topographic features and methane seepage appears to influence food supply for macrofauna and microbes in ways that supersede any clear depth gradient in organic matter input. The availability of organic C and the abundance of microorganisms in the upper sediment (1–5 cm) are correlated. Nutritional patterns in fauna reflect considerable small-scale heterogeneity in food sources. We speculate that the occurrence of high densities of *Elphidium*, a typically shallow-water foraminiferan, results from the influence of sediment redeposition from shallower habitats (e.g., turbidity current sedimentation). Macrofauna from clam bed and pogonophoran field seep patches exhibit distinct chemosynthetic inputs to the carbon pool.

We report the first seep on the central Aleutian slope in the Unimak region, with distinct assemblages inhabiting clam bed, pogonophoran field and carbonate habitats. Our observations suggest key roles for sediment instability, and the porosity of sedimentary rocks through which fluids can migrate in promoting chemosynthetic communities. Such seep 'patches' are likely to be widespread across the bathyal Aleutian margin. The Unimak seep fauna was distinctive in its high representation of crustaceans. We hypothesize this reflects relatively low levels of sulfide and possibly limited methane flux rates in Unimak sediments, as well as some degree of sediment instability. Another distinctive feature was the high cover and high density of epibenthic megafauna on rocks near the Unimak seepage site, suggesting a heretofore unexplored nutritional influence of methane seepage on reef faunas.

The overall picture of the mid Aleutian slope is one of extensive geological, biogeochemical and biological heterogeneity. This heterogeneity, combined with pervasive physical and sediment disturbance features is characteristic of continental slopes worldwide (Masson et al., 1996) and is likely to be one explanation for the exceptionally high biodiversity characteristic of the world's continental margins (Rex et al., 1997; Levin et al., 2001).

Acknowledgments

We thank the Captain and crew of the Revelle leg KRUSO3RR, the JASON II team and participating scientists for facilitating work at sea. We thank Jesse Leddick, Michelle Abriani, Amanda Shepherd, Brian Wrightsman and Jennifer Do for help at sea, Jennifer Gonzalez for laboratory assistance with isotope sample preparation and David Harris (UC Davis) and Robert Michener (U Mass Boston) for conducting stable isotope analyses of macrofauna, and Marylin Fogel (Carnegie Institute Washington) for isotope analyses on sediment samples. Larry Lovell and the SIO benthic invertebrate collection provided assistance with faunal identifications. Randa I. Abboud, Lauren E. Lewis and Darrell Atkinson (USC) provided for assistance with sediment analyses and bacterial counts. Support for the research was provided by the NOAA West Coast National Undersea Research Center (UAF 04-0111 to A.E.R.;

UAF 04-0112 to L.A.L.; UAF 04-0109 to J.B.M.; UAF 04-0107 to G.J.F.).

References

Basak, C., Rathburn, A.E., Pérez, M.E., Martin, J.B., Kluesner, J.W., Levin, L.A., De Deckker, P., Gieskes, J.M., Abriani, M. (2009) Carbon and oxygen isotope geochemistry of live (stained) benthic foraminifera from the Aleutian Margin and the southern Australian Margin. Marine Micropaleontology, in press, doi:10.1016/j.marmicro.2008.11.002..

Beaulieu, S.E., 2001. Colonization of habitat islands in the deep sea: recruitment to glass sponge stalks. Deep-Sea Research I 48 (4), 1121–1137.

Bernal, P., Ahumada, R., González, H., Pantoja, S., Troncoso, A., 1989. Carbon flux in a pelagic trophic model to Concepción bay, Chile. Biología Pesquera 18, 5–14.

Belyaev, G.M., 1966. Bottom fauna of the ultra-abyssal depths of the world ocean. Akad. Nauk SSSR, Trudy Inst. Okeanol. 591, 1–248 (in Russian).

Bernhard, J.M., 2000. Distinguishing live from dead foraminifera: methods review and proper applications. Micropaleontology 46 (Suppl. 1), 38–46.

Bernhard, J.M., Ostermann, D.R., Williams, D.S., Blanks, J.K., 2006. Comparison of two methods to identify live benthic foraminifera: a test between Rose Bengal and CellTracker Green with implications for stable isotope paleoreconstructions. Paleoceaongraphy 21, PA4210. doi:10.1029/2006PA001290.

Boon, A.R., Duineveld, G.C.A., 1996. Phytopigments and fatty acids as molecular markers for the quality of near-bottom particulate organic matter in the North Sea. Journal of Sea Research 34, 279–291.

Caress, D.W., Chayes, D.N., 1995. New software for processing sidescan data from sidescan-capable multibeam sonars. In: Proceedings of the IEEE Oceans 95 Conference, pp. 997–1000.

Caress, D.W., Chayes, D.N., 1996. Improved processing of Hydrosweep DS multibeam data on the R/V Maurice Ewing. Marine Geophysical Research 18, 631–650.

Corliss, B.H., 1991. Morphology and microhabitat preferences of benthic foraminifera form the northwest Atlantic Ocean. Marine Micropaleontology 17, 195–236.

DeMets, C., Dixon, T.H., 1999. New kinematic models for Pacific-North America motion from 3 Ma to present: I, evidence for steady motion and biases in the NUVEL-1A model. Geophysical Research Letters 26 (13), 1921–1924.

Dobson, M.R., Karl, H.A., Vallier, T.L., 1996. Sedimentation along the fore-arc region of the Aleutian island arc Alaska. In: Gardner, V., Field, M.E., Twichell, D.C. (Eds.), Geology of the United States' Seafloor; The View from GLORIA. Cambridge University Press, Cambridge, UK.

Edmond, J., 1974. On the dissolution of carbonate and silicate in the deep ocean. Deep-Sea Research 21 (6), 455–480.

Epstein, S.S., Rossel, J., 1995. Enumeration of sandy sediment bacteria: search for optimal protocol. Marine Ecology Progress Series 117, 289–298.

Fontanier, C., Jorissen, F.J., Chaillou, G., David, C., Anschutz, P., Gremare, A., Griveaud, C., 2005. Live foraminiferal faunas from a 2800 m deep lower canyon station from the Bay of Biscay: faunal response to focusing of refractory organic matter. Deep-Sea Research I 52, 1189–1227.

Friedman, I., O'Neil, J.R., 1977. Compilation of stable isotope fractionation factors of geochemical interest: U.S. Geological Survey Professional Paper 440-KK.

Fryer, G.J., Tryon, M.D., 2005. Great earthquakes, gigantic landslides, and the continuing enigma of the April Fool's tsunami of 1946. EOS Transactions AGU 86 (52). T11A-0355.

Fryer, G.J., Watts, P., Pratson, L.F., 2004. Source of the great tsunami of 1 April 1946: a landslide in the upper Aleutian forearc. Marine Geology 204, 201–218.

Gage, J.D., Tyler, P.A., 1999. Deep-sea biology: a natural history of organisms at the deep-sea floor. Cambridge University Press, Cambridge, UK.

Gieskes, J.M., Gamo, T., Brumsack, H., 1991. Chemical Methods for Interstitial Water Analysis on board Joides Resolution. Ocean Drilling Program Technical Reports, 15.

Gieskes, J., Mahn, C., Day, S., Martin, J.B., Greinert, J., Rathburn, A., MacAdoo, B., 2005. A study of the chemistry of pore fluids and authigenic carbonates in methane seep environments: Kodiak Trench, Hydrate Ridge, Monterey Bay, and Eel River Basin. Marine Chemistry 220 (3–4), 329–345.

Glud, R.N., Gundersen, J.K., Jørgensen, B.B., Revsbech, N.P., Schulz, H.D., 1994. Diffsuive and total oxygen uptake of deep-sea sediments in the Eastern South Atlantic Ocean: in-situ and laboratory measurements. Deep-Sea Research 41, 1767–1788.

Goldstein, S.T., Corliss, B.H., 1994. Deposit feeding in selected deep-sea and shallow-water benthic foraminifera. Deep-Sea Research 41 (2), 229–241.

Gooday, A.J., 1999. Biodiversity of foraminifera and other protists in the deep sea: scales and patterns. Belgium Journal of Zoology 129 (1), 61–80.

Gooday, A.J., 2002. Organic-walled allogromiids: aspects of their occurrence, diversity and ecology in marine habitats. Journal of Foraminiferal Research 32, 384–399.

Gooday, A.J., Levin, L.A., Linke, P., Heeger, T., 1992. The role of benthic foraminifera in deep-sea food webs and carbon cycling. In: Rowe, G.T., Pariente, V. (Eds.), Deep-sea Food Chains and the Global Carbon Cycle. Kluwer Academic Publishers, The Netherlands, pp. 63–91.

Gooday, A.J., Nomaki, H., Kitazato, H., 2008. Modern deep-sea benthic foraminifera: a brief review of their morphology-based biodiversity and trophic diversity. Geological Society, vol. 303, Special Publications, London, pp. 97–119. 10.1144/SP303.8.

Gundersen, J.K., Jørgensen, B.B., 1990. Microstructure of diffusive boundary layer and the oxygen uptake of the sea floor. Nature 345, 604–607.

Hecker, B., Logan, D.T., Gandarillas, F.E., Gibson, P.R., 1983. Megafaunal assemblages in canyon and slope habitats. In: Canyon and Slope Processes Study. Final Report prepared for U.S. Department of the Interior, Minerals Management Service, Washington, DC, US Department of Interior, vol. III, Chapter I (Contract 14-12-0001-29178), Palisades, NY, pp. 1–140.

Heezen, B.C., Hollister, C.D., 1971. The Face of the Deep, 659. Oxford University Press, New York.

Holby, O., Ries W., 1996. In situ oxygen dynamics and profiles. In: Schulz H.D., Cruise Participants, Report and preliminary results of Meteor cruise M34/2 Walvis Bay – Walvis Bay, 1996 Berichte, Fachbereich Geowissenschaften, University of Bremen, vol. 78, pp. 85–87.

Jeroschewsky, P., Steuckart, C., Kuehl, M., 1996. An amperometric microsensor for the determination of H_2 S in aquatic environments. Analytical Chemistry 68, 4351–4357.

Jørgensen, B.B., Revsbech, N.P., 1985. Diffusive boundary layers and the oxygen uptake of sediments and detritus. Limnology and Oceanography 30, 111–122.

Jorissen, F., 1999. Benthic foraminiferal microhabitats below the sediment–water interface. In: Sen Gupta, B. (Ed.), Modern Foraminifera. Academic Publishers, pp. 181–199.

Jumars, P.A., Hessler, R.R., 1976. Hadal community structure: implications from the Aleutian Trench. Journal of Marine Research 34, 547–560.

Levin, L.A., Gooday, A., 2003. The Atlantic. In: Tyler, P. (Ed.), Ecosystems of the World: The Deep Sea. Elsevier, Amsterdam, pp. 111–178.

Levin, L.A., Gooday, A.J., James, D., 2001. Dressing up for the deep: agglutinated protozoans adorn an irregular urchin. Journal of the Marine Biological Association UK 81, 881–882.

Levin, L.A., Mendoza, G., 2007. Community structure and nutrition of deep methane seep macroinfauna from the Aleutian Margin and Florida Escarpment, Gulf of Mexico. Marine Ecology 28, 131–151.

Levin, L.A., Ziebis, W., Mendoza, G.F., Growney-Cannon, V., Walther, S., 2006. Recruitment response of methane-seep macrofauna to sulfide and surrounding habitat. Journal of Experimental Marine Biology and Ecology 330, 132–150.

Lewis, S.D., Ladd, J.W., Burns, T.R., 1988. Structural development of an accretionary prism by thrust and strike-slip faulting: Shumagin region, Aleutian Trench. Geological Society of America Bulletin 100, 767–782.

Lundsten, L., Barry, J.P., Cailliet, G.M., Clague, D.A., DeVogelaere, A.P., Geller, J.B., 2009. Benthic invertebrate communities on three seamounts off Southern and Central California, USA. Marine Ecology Progress Series 374, 23–32.

MacAvoy, S.E., Carney, R.S., Fisher, C.R., Macko, S.A., 2002. Use of chemosynthetic biomass by large, mobile benthic predators in the Gulf of Mexico. Marine Ecology Progress Series 225, 65–78.

Mackensen, A., Wollenburg, J., Licari, L., 2006. Low δ^{13} C in tests of live epibenthic and endobenthic foraminifera at a site of active methane seepage. Paleoceanography 21, PA2022. doi:10.1029/2005PA001196.

Martin, J.B., Day, S., Rathburn, A.E., Pérez, M.E., Mahn, C., Gieskes, J.M., 2004. Do fossil foraminifera record isotopically light carbon at cold seeps? Geochemistry, Geophysics and Geosystems 5 (4), Q04004. doi:10.1029/2003GC000629.

Masson, D.G., Kenyon, N.H., Weaver E., P.P., 1996. Slides, debris flows and turbidity currents. In: Summerhayes, C.P., Thorpe, S.A. (Eds.), Oceanography: An illustrated Guide. Wiley, London, pp. 136–151.

McClain, C.R., Rex, M.A., Johnson, N., 2004. Morphological disparity as a biodiversity metric in lower bathyal and abyssal gastropod assemblages. Evolution 58, 338–348.

McCorkle, C.D., Keigwin, L.D., Corliss, B.H., Emerson, S.R., 1990. The influence of microhabitats on the carbon isotopic composition of deep-sea benthic foraminifera. Paleoceanography 5 (2), 161–185.

McCorkle, D.C., Corliss, B.H., Farnham, C.A., 1997. Vertical distributions and stable isotopic compositions of live (stained) benthic foraminifera from the North Carolina and California continental margins. Deep-Sea Research Part I: Oceanographic Research Papers 44 (6), 983–1024.

Meyer-Reil, L., 1983. Benthic response to sedimentation events during autumn to spring at shallow water station in the western Kiel Bight. Marine Biology 77, 247–256.

Mordy, C.W., Stabeno, P.J., Ladd, C., Zeeman, S., Wisegarver, D.P., Salo, S.A., Hunt, G.L., 2005. Nutrients and primary production along the eastern Aleutian Island Archipelago. Fisheries Oceanography 14 (Sl), 55–76.

Murray, J.W., Bowser, S.S., 2000. Mortality, protoplasm decay rate, and reliability of staining techniques to recognize 'living' foraminifera: a review. Journal of Foraminiferal Research 30 (1), 66–70.

Paull, C.K., Schlining Usler, W., Paduan, J.B., Caress, D., Greene, H.G., 2005a. Distribution of chemosynthetic biological communities in Monterey Bay, California. Geology 33, 85–88.

Paull, C.K., Ussler, W., Greene, H.G., Barry, J., Keaten, R., 2005b. Bioerosion by chemosynthetic biological communities on Holocene submarine slide scars. Geo-Marine Letters 25, 11–19.

Pfannkuche, O., 1993. Benthic response to the sedimentation of particulate organic matter at the BIOTRANS station 47°N, 20°W. Deep-Sea Research I 40, 135–149.

Pfannkuche, O., Soltwedel, T., 1998. Small benthic size classes along the N > W. European continental margin: spatial and temporal variability in activity and biomass. Progress in Oceanography 42, 189–207.

Plante-Cuny, M.R., 1973. Reserches sur la production primaire bentique en milieu marin tropical I Variations de la production primaire et des teneurs en pigments photosynthétiques sur quelques fonds sableux. Valeur des résultats obtenus par la méthode du^{14} C, 11, 317–348.

Rathburn, A.E., Corliss, B.H., 1994. The ecology of deep-sea benthic foraminifera from the Sulu Sea. Paleoceanography 9, 87–150.
Rathburn, A.E., Corliss, B.H., Tappa, K.D., Lohmann, K.C., 1996. Comparisons of the ecology and stable isotopic compositions of living (stained) deep-sea benthic foraminifera from the Sulu and South China Seas. Deep-Sea Research 43 (10), 1617–1646.
Rathburn, A.E., Perez, M.E., Martin, J.B., Day, S.A., Mahn, C., Gieskes, J., 2003. Relationships between the distribution and stable isotopic signatures of living foraminifera and cold seep biogeochemistry in Monterey Bay, California. Geochemistry, Geophysics and Geosystems 4, 1106. doi:10.1029/2003GC000595, 1–28.
Revsbech, N., 1989. An oxygen sensor with a guard cathode. Limnology and Oceanography 31, 305–318.
Revsbech, N., Jørgensen, B., 1986. Microelectrodes: their use in microbial ecology. Advances in Microbiology and Ecology 9, 63–72.
Rex, M.A., Etter, R.J., Morris, J.S., Crouse, J., McClain, C.R., Johnson, N.A., Stuart, C.T., Deming, R.T., Thies, R., Avery, R., 2006. Global bathymetric patterns of standing stock and body size in the deep-sea benthos. Marine Ecology Progress Series 317, 1–8.
Rex, M.A., Stuart, C.T., Etter, R., 1997. Large-scale patterns of species diversity in the deep-sea benthos. In: Ormon, R., Gage, J.D., Angel, M.V. (Eds.), Marine Biodiversity: Patterns and Processes. Cambridge University Press, Cambridge, UK, pp. 94–121.
Risgaard-Petersen, N., Langezaal, A.M., Ingvardsen, S., Schmid, M.C., Jetten, M.S., Op den Camp, H.J., Derksen, J.W., Pina-Ochoa, E., Eriksson, S.P., Nielsen, L.P., Revsbech, N.P., Cedhagen, T., van der Zwaan, G.J., 2006. Evidence for complete denitrification in abenthic foraminifer. Nature 443 (7107), 93–96.
Snelgrove, P.V.R., Grassle, J.F., Petrecca, R.F., 1994. Macrofaunal response to artificial enrichments and depressions in a deep-sea habitat. Journal of Marine Research 52, 345–369.
Snider, L.J., Burnett, B.R., Hessler, R.R., 1984. The composition and distribution of meiofauna and nanobiota in a central North Pacific deep-sea area. Deep-Sea Research 31, 1225–1249.
Suess, E., 1980. Particulate organic carbon flux in the ocean – surface productivity and oxygen utilization. Nature 28S, 260–263.
Suess, E., Bohrmann, G., 1997. FS SONNE cruise report, SO110: SO-RO (SONNE-ROPOS), Victoria-Kodiak-Victoria, July 9–August 19, 1996. GEOMAR Rpt., 59:181.
Vetter, E.W., 1995. Detritus-based patches of high secondary production in the nearshore benthos. Marine Ecology Progress Series 120, 251–262.
Wallmann, K., Linke, P., Suess, E., Bohrmann, G., Sahling, H., Schluter, M., Dahlmann, A., Lammers, S., Greinert, J., von Mirach, N., 1997. Quantifying fluid flow, solute, mixing and biogeochemical turnover at cold vents of the eastern Aleutian subduction zone. Geochimica et Cosmochimica Acta 61, 5209–5219.
Wessel, P., Smith, W.H.F., 1991. Free software helps map and display data. EOS, Transactions, AGU, 72, 441.
Ziebis, W., Haese, R.R., 2005a. Interactions between fluid flow, geochemistry and biogeochemical processes at methane seeps. In: Kristensen, E.J.K., Haese, R.R. (Eds.), Macro and Microorganisms in Marine Sediments, AGU Coastal and Estuarine Studies 60, 267–298.
Ziebis, W., Jacobson, M., Capone, D.G., Fuhrman, J. A., Hewson, I., Rathburn, A.E., 2005. Comparison of microbial activity and diversity in deep-sea sediments at the Unimak Margin, Alaska. Abstract, American Society Limnology and Oceanography, Salt Lake City, February, 20–25.